Supporting Information for:

CO_2-driven stereochemical inversion of sugars to create thymidine-based polycarbonates by ring-opening polymerisation

Georgina L. Gregory,[a] Elizabeth M. Hierons,[a] Gabriele Kociok-Köhn,[a] Ram Sharma,[b] and Antoine Buchard[a,*]

[a] Department of Chemistry, University of Bath, Bath BA2 7AY
a.buchard@bath.ac.uk

[b] Department of Chemical Engineering, University of Bath, Bath BA2 7AY

Table of Contents

1. Experimental Details

1.1 Materials

Thymidine was purchased from Carbosynth and used without further purification. Anhydrous acetonitrile and 1,5,7-triazabicyclo[4.4.0] dec-5-ene (TBD) were purchased from Sigma Aldrich. TBD was dried over CaH_2 immediately prior to use by dissolution in dry THF. 4-Methyl benzyl alcohol was purchased from Acros Organics, recrystallised from dry diethyl ether and stored in a glovebox prior to use. Dry THF and dry diethyl ether were obtained from an MBraun solvent purification system (SPS) and stored over 3Å molecular sieves. N4.5 CP grade CO_2 was purchased from BOC and introduced by fitting the gas cylinder to a Schlenk line and using standard Schlenk line techniques. Column chromatography was performed on silica gel (200-400 mesh particle size, 60 Å pore size), purchased from Sigma Aldrich. Spots were visualised under UV light before staining with $KMnO_4$ solution. All other reagents were purchased from either Sigma Aldrich or Alfa Aesar and used without further purification. MG-63 cells were purchased from Sigma-Aldrich.

1.2 Methods

All polymerisations were carried out under an argon atmosphere using standard Schlenk line techniques. All ***NMR spectra*** were recorded in $CDCl_3$, MeCN-d_3 or D_2O on a Bruker-400 instrument and referenced to residual solvent peaks: ^{1}H NMR spectra (400 MHz) δ_H = 7.26 ($CDCl_3$), 1.94 (MeCN-d_3) and 4.79 ppm (D_2O); $^{13}C\{^{1}H\}$ spectra (101 MHz) δ_C = 77.16 (CDCl3) and 118.26 ppm (MeCN-d_3). Coupling constants are reported in Hertz. Polymer conversions were determined by ^{1}H NMR spectroscopy

(400 MHz, $CDCl_3$). ***CHN microanalysis*** was performed by Mr Stephen Boyer of the London Metropolitan University. ***Melting points*** were measured on a variable temperature Griffin melting point apparatus. ***Mass spectrometry*** were recorded with a microToF electrospray time-of-flight (ESI-ToF) mass spectrometer (Bruker Daltonik) in methanol, acetonitrile or water. ***Infra-red spectra*** were recorded as thin films on a Perkin-Elmer 1600 Fourier transform spectrometer. Number-average molecular weight M_n and dispersities Đ (M_w/M_n) were estimated by ***size exclusion chromatography (SEC)*** with a differential refractive index (RI) detector (maintained at 35 °C) using the 1260 SEC MDS system from Agilent. The PL gel 5µm mixed-D 300x7.5 mm column and 5µm PLgel 50x7.5 mm guard column were calibrated with a set of polystyrene standards. HPLC grade $CHCl_3$ (1 mL min^{-1}) was used as the mobile phase and polymeric samples dissolved at a concentration of 2 mg mL^{-1}. Glass transition temperatures (T_g) were measured by ***differential scanning calorimetry (DSC)*** using a MicroSC multicell calorimeter from Setaram; the Calisto program was employed to collect and process the data. Both measurement and reference cells were 1 mL Hastelloy C cells, roughly 5-10 mg of polymeric material was loaded into the measurement cell with the reference cell left empty. The experiment was performed under nitrogen gas and the sample heated from 20 to 200 °C at a rate of 1 K min^{-1} and then cooled at the same rate. A second heating and cooling cycle was carried out immediately following completion of the first. A Setsys Evolution TGA 16/18 from Setaram was used for ***thermogravimetric analysis (TGA)***; the Calisto program was employed to collect and process the data. The sample was loaded into a 170 µL alumina crucible and the analytical chamber purged with argon (200 mL min^{-1}) for 40 min prior to starting the analysis. The sample was then heated under an argon flow (20 mL min^{-1}) from 30 to 500 °C at a rate of 5 K min^{-1}. During the heating ramp, evolving gas was taken off from the analytical chamber to a mass spectrometer through a stainless steel capillary. The mass spectrometer was a Omnistar GSD 320 by Pfeiffer Vacuum, equipped with a quadrupole mass analyser and a SEM detector. ***Matrix-assisted laser desorption ionisation-time of flight (MALDI-ToF)*** mass spectrometry was conducted using a Bruker Autoflex speed MALDI Mass Spectrometer equipped with a 2 kHz Smartbeam-II laser. A solution of trans-2-[3-(4-tert-butylphenyl)-2-methyl-2-propenylidene]malononitrile (DCTB) matrix in $CHCl_3$ (10 mg mL^{-1}) was added to $CHCl_3$ solutions of polymer (5 mg mL^{-1}) with sodium trifluoroacetate (0.1 M in HFIP) in

a 25:5:1 ratio, and the samples centrifuged for 1 min. A micropipette was used to spot ~1 μL of the solution onto a polished steel MALDI plate and the solvent allowed to evaporate in air. Once loaded, positive ion MALDI spectra were obtained in reflector mode. Laser intensity was varied. The data was analysed using the Flex Analysis software, version 3.4 (build 76). The molecular weight distributions and percentage of each species present were obtained through analysis of the data in the Polytools software package 1.31. All **single-crystal X-ray diffraction** analysis was carried out by Dr Gabriele Kociok-Kohn on a Nonius Kappa CCD diffractometer using Cu-K_α radiation (λ = 1.54184 Å) at 150 K. ***Powder diffraction patterns*** were recorded by Dr Gabriele Kociok-Kohn on a Bruker Advance D8 diffractometer with copper K_α radiation (λ = 1.5406 Å) at 298 K. The sample was ground with a pestle and mortar before being transferred to a disk. Data was recorded from a 2θ of 4 to 60° with 0.02 steps s^{-1} and 0.5 s $step^{-1}$. **Contact Angles** were measured with the DataPhysics OCA_{50} micro instrument. 2 μL water droplets were dropped onto the polymer surface and the SCA20 software package used to measure both the right and left contact angles. Polymer films were prepared by drop-casting 1 wt% polymer solutions in CH_2Cl_2 onto glass slides and allowing the solvent to evaporate before drying in a vacuum oven overnight at 40 °C.10 measurements were recorded for 3 polymer films and compared to the glass slide as a control and films of the monomer prepared in the same manner. **Cell attachment studies** were performed with the MG-63 bone cancer cell line. These were maintained in corning T75 cell culture flasks at 37 °C in FBS^+ growth medium (87 v/v% Dulbecco's Modified Eagle Medium, 10% fetal bovine serum (FBS), 1% penicillin streptomycin, 1% non-essential amino acids and 1% sodium pyruvate). Cells were passage every 4 days by removing the growth medium and washing with phosphate-buffered saline (PBS) solution (10 ml) before treatment with trypsin (5 ml) to detach the cells from the culture flask. The trypsin was removed by centrifugation (1000 rpm, 15 minutes) in growth media (10 ml) and the cell sediment then re-suspended in fresh growth media (10 ml). Following staining of the cell suspension (100 μL) with trypan blue (100 μL), the number of live cells was counted with a Luna dual fluorescence cell counter immediately prior to attachment studies. Thin films were prepared by drop casting polymer solutions in CH_2Cl_2 (as for the contact angle measurements detailed above) of 0.25, 0.5, 0.75 and 1 wt% onto glass slides. These were sterilised with 70% EtOH (aq) and glued into the wells of a Corning Costar 24 cell culture plate with

Norland Optical Adhesive 63, set and further sterilised under UV light in a Heoroff UV 500 crosslinker at 100 μJ cm^{-2} for 15 minutes. After washing the wells with PBS solution (0.5 ml), cells were seeded in growth media (0.5 ml) at a density of 10, 000 live cells cm^{-2}. 3 repeats were performed for each polymer wt% and compared to empty wells and glass controls. After 1 or 24 h incubation periods at 37 °C, the media was removed and each well washed with PBS solution (2 × 0.5 ml). Attached cells were fixed with formalin solution (0.5 ml, 10% formaldehyde, 90% PBS). After 15 minutes, this was removed and the wells washed with PBS solution (2 × 0.5 ml) before staining with 4,6-diamidino-2-phenylindole (DAPI) solution (150 μL, 0.002% DAPI in PBS). The solution was removed after 15 minutes and any residual fluorescent staining agent removed by washing with PBS solution (2 × 0.5 ml). Care was taken to ensure minimum light exposure during the staining procedure. Cell images were recorded using a EVOS digital optical microscope under low light at 10x objective. 6 images were recorded at different locations for each well plate and images analysed using ImageJ software 1.7.0_55 (32-bit) to determine the cell count.

1.3 Monomer Synthesis

3'-tosyl-5'-TBDMS-thymidine (4)

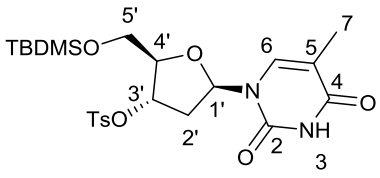

In a modified literature procedure,[11] under a stream of argon, *t*-$BuMe_2SiCl$ (TBDMSCl) (6.16 g, 40.9 mmol, 1.1 equiv.) was added portion-wise to a solution of thymidine (9.00 g, 37.2 mmol, 1 equiv.) and DMAP (0.454 g, 3.72 mmol, 0.1 equiv.) in anhydrous pyridine (45 ml). The reaction mixture was stirred at room temperature and progress monitored by TLC (5'-TBDMS-thymidine R_f 0.60 in 9:1 $CHCl_3$: EtOH). After 48 h, TsCl (7.79 g, 40.9 mmol, 1.1 equiv.) was added and the reaction stirred for a further 48h at room temperature until TLC analysis showed consumption of the 5'-silyl thymidine. The reaction mixture was quenched by addition of methanol and the solvent removed *in vacuo*. The crude material was then extracted into $CHCl_3$, washed with H_2O and dried over $MgSO_4$. Recrystallisation from hot ethanol afforded a white crystalline solid (15.9 g, 84%). **R_f** 0.77 (9:1 $CHCl_3$: EtOH); **Found:** C, 54.05; H, 6.79; N, 5.47. $C_{23}H_{34}N_2O_7SSi$ requires C, 54.10; H, 6.71; N, 5.49%; **δ_H (400 MHz, $CDCl_3$):** 8.57 (1H, s, NH), 7.80 (2H, d, *J* 8.4 Hz, TsPh), 7.38 (3H, m, TsPh + 6-H), 6.30 (1H, dd, *J* 9.0, 5.4 Hz, H-1'), 5.06 (1H, d, *J* 6.3 Hz, H-3'), 4.26 (1H, q, *J* 2.0 Hz, H-

4'), 3.85 (1H, dd, *J* 11.5, 2.0 Hz, H-5'), 3.73 (1H, dd, *J* 11.5, 2.0 Hz, H-5'), 2.46 (3H, s, TsMe), 2.41 (1H, ddd, *J* 14.1, 5.4, 1.1 Hz, H-2'), 2.02 (1H, ddd, *J* 14.1, 9.0, 6.3 Hz, H-2'), 1.89 (3H, d, *J* 1.2 Hz, Me-7), 0.90 (9H, s, ^{t}BuSi), 0.09 (6H, d, *J* 0.5 Hz, Me_2Si); **δ_C (101 MHz, $CDCl_3$):** 163.7 (C-4), 150.3 (C-2), 145.6 (C-6), 134.9, 133.5, 130.2, 128.0 (Ar-H), 111.4 (C-5), 85.1 (C-4'), 84.6 (C-1'), 80.8 (C-3'), 63.1 (C-5'), 38.6 (C-2'), 26.0 ($C(\underline{C}H_3)_3Si$), 21.8 (TsMe), 18.4 ($\underline{C}(CH_3)_3Si$), 12.6 (C-7), -5.27 (Me_2Si), -5.44 (Me_2Si); **HR-MS (ESI)** $[C_{23}H_{34}N_2O_7SSi + Na]^+$ Theo. 533.1754 found 533.1739.

3-N-methyl-3'-tosyl-5'-TBDMS-thymidine (3)

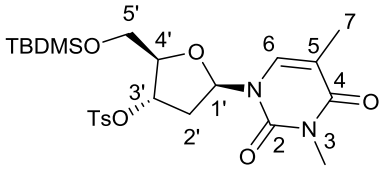

Following a procedure for the methylation of thymidine,[1] MeI (18.3 ml, 294 mmol, 10 equiv.) was added to a suspension of K_2CO_3 (20.3 g, 147 mmol, 5 equiv.) and 3'-tosyl-5'-TBDMS thymidine **4** (15.0 g, 29.4 mmol, 1 equiv.) in acetone (290 ml) and the reaction mixture stirred at room temperature. After 24 h, excess K_2CO_3 was removed by filtration and volatiles removed *in vacuo*. Recrystallisation from hot ether afforded large colourless blocks (14.5 g, 93%). **R_f** 0.68 (1:1 acetone: $CHCl_3$); **Found:** C, 54.99; H, 6.85; N, 5.44. $C_{24}H_{36}N_2O_7SSi$ requires C, 54.94; H, 6.90; N, 5.34%; **δ_H (400 MHz, $CDCl_3$)** 7.79 (2H, d, *J* 8.4 Hz, TsPh), 7.37 (3H, m, TsPh + H-6), 6.33 (1H, dd, *J* 8.9, 5.4 Hz, H-1'), 5.06 (1H, d, *J* 6.4 Hz, H-3'), 4.26 (1H, q, *J* 2.0, H-4'), 3.84 (1H, dd, *J* 11.5, 2.0, H-5'), 3.72 (1 H, dd, *J* 11.5, 2.0, H-5'), 3.31 (3 H, s, 3-Me), 2.46 (3 H, s, TsMe), 2.43 (1 H, dd, *J* 14.3, 8.9, 5.4, H-2'), 2.01 (1 H, ddd, *J* 14.3, 8.9, 6.4, H-2'), 1.90 (3 H, d, *J* 1.2, 7-Me), 0.89 (9 H, s, ^{t}BuSi), 0.09 (6 H, d, *J* 1.0, Me_2Si); **δ_C (101 MHz, $CDCl_3$)** 163.6 (C-4), 151.1 (C-2), 145.6 (C-6), 133.5, 132.7, 130.2, 128.0 (TsPh), 110.4 (C-5), 85.4 (C-4'), 85.0 (C-1'), 80.8 (C-3'), 63.1 (C-5'), 38.7 (C-2'), 28.0 (3-Me), 26.0 ($(CH_3)_3C$), 21.8 (TsMe), 18.4 ($C(CH_3)_3$), 13.4 (7-Me), -5.3 (Me_2Si), -5.5 (Me_2Si); **HR-MS (ESI)** $[C_{24}H_{36}N_2O_7SSi + Na]^+$ Theo. 547.1910 found 547.1908.

3-N-methyl-3'-tosyl-thymidine (2)

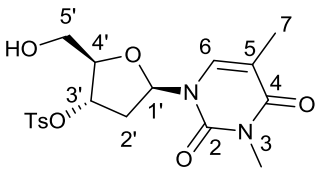

Following the procedure outlined by Vaino and Szarek,[14] a 0.1 mol L^{-1} solution of 3-*N*-methyl-5'-TBDMS-3'-tosyl-thymidine **3** (12.6 g, 24 mmol, 1 equiv.) in methanol was treated with 1

wt% iodine and the reaction mixture heated to reflux for 2 h (monitored by TLC 1:1 acetone:$CHCl_3$). After cooling to room temperature, excess iodine was quenched with sodium thiosulfate until colourless. Volatiles were removed under reduced pressure and the residue extracted into EtOAc, washed with water and the organic layer dried over $MgSO_4$. Recrystallisation from hot EtOH afforded large colourless crystals suitable for single-crystal X-ray analysis (9.36 g, 95%). **R_f** 0.60 (1:1 acetone: $CHCl_3$); **Found:** C, 52.71; H, 5.41; N, 6.90. $C_{18}H_{22}N_2O_7S$ requires C, 52.69; H, 5.40; N, 6.93%; **δ_H (400 MHz, $CDCl_3$)** 7.82 – 7.75 (2H, m, Ar-H), 7.39 – 7.34 (2H, m, Ar-H), 7.32 (1H, d, *J* 1.2 Hz, H-6), 6.06 (1H, dd, *J* 8.4, 6.0 Hz, H-1'), 5.19 (1H, dt, *J* 6.4, 2.2 Hz, H-3'), 4.21 (1H, q, *J* 2.3 Hz, H-4'), 3.83 (1H, ddd, *J* 12.0, 3.3, 2.2 Hz, H-5'), 3.68 (1H, ddd, *J* 12.0, 6.9, 2.2 Hz, H-5'), 3.28 (3H, s, 3-Me), 3.07 (1H, dd, *J* 6.9, 3.3 Hz, 5'-OH), 2.49 (1H, ddd, *J* 14.3, 8.4, 6.4 Hz, H-2'), 2.44 (3H, s, TsMe), 2.35 (1H, ddd, *J* 14.3, 6.0, 2.1 Hz, H-2'), 1.89 (3H, d, *J* 1.2 Hz, 7-Me); **δ_C (101 MHz, $CDCl_3$)** 163.6 (C-4), 151.1(C-2), 145.6 (C-6), 135.0, 133.3, 130.2, 127.9 (Ar-C), 110.5 (C-5), 88.3 (C-1'), 85.0 (C-4'), 80.8 (C-3'), 62.2 (C-5'), 37.5 (C-2'), 28.0 (3-Me), 21.8 (TsMe), 13.3 (7-Me); **HR-MS (ESI)** $[C_{18}H_{22}N_2O_7S + Na]^+$ Theo. 433.1045 m/z found 433.1047 m/z.

Cyclic 3-N-methyl-3',5'-O-cis-carbonate-thymidine (1)

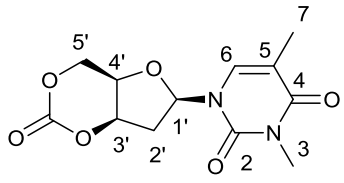

Under an inert atmosphere, 3-*N*-methyl-3'-tosyl-thymidine **2** (6.16 g, 15 mmol, 1 equiv.) was dissolved in anhydrous acetonitrile (150 ml, 0.1 M). After three cycles of vacuum followed by CO_2, the solution was saturated with CO_2 at 0°C in an ice-water bath. Under a stream of CO_2, DBU (2.2 ml, 15 mmol, 1 equiv.) was added dropwise and the solution allowed to warm to room temperature before being slowly heated to 40 °C. The reaction was monitored by NMR spectroscopy and after 48 h volatiles were removed under reduced pressure and the reaction mixture immediately subjected to column chromatography (9:1 $CHCl_3$: acetonitrile). Recrystallised from hot anhydrous toluene gave colourless needles suitable for single-crystal X-ray diffraction (2.20 g, 52%). **R_f** 0.35 (1:1 acetone: $CHCl_3$); **Found:** C, 51.09; H, 4.94; N, 9.94. $C_{12}H_{14}N_2O_6$ requires C, 51.07; H 5.00; N 9.93%. **δ_H (400 MHz, $CDCl_3$)** 7.19 (1H, q, *J* 1.2 Hz, H-6), 6.37 (1H, dd, *J* 8.1, 4.3 Hz, H-1'), 5.15 (1 H, ddd, *J* 5.6, 3.9, 1.3 Hz, H-3'), 4.69 (1 H, dd, *J* 12.8, 1.8 Hz, H-5'), 4.60 (1 H, dd, *J* 12.8, 2.4 Hz, H-5'), 4.35 (1 H, ddd, *J* 3.9, 2.4, 1.8 Hz, H-4'), 3.34 (3 H, s, 3-Me), 2.90 (1 H, ddd, *J* 15.9, 8.1, 5.6 Hz, H-2'),

2.40 (1 H, ddd, *J* 15.9, 4.3, 1.3 Hz, H-2'), 1.95 (3 H, d, *J* 1.2 Hz, 7-Me); **δ_C (101 MHz, $CDCl_3$)** 163.3 (C-4), 151.3 (C-2), 147.0 (C=O), 131.9 (C-6), 111.4 (C-5), 84.6 (C-1'), 79.5 (C-3'), 72.1 (C-4'), 66.9 (C-5'), 39.9 (C-2'), 28.0 (3-Me), 13.4 (7-Me). **HR-MS (ESI)** $[C_{12}H_{14}N_2O_6 + Na]^+$ Theo. 305.0736 found 305.0749; **FTIR** (thin film) cm^{-1} 1749, 1702, 1673, 1637 (3 C=O, C=C); **Mpt.** 204-205 °C.

Cyclic 3-N-benzoyl- 3',5'-O-cis-carbonate-thymidine (1-Bz)

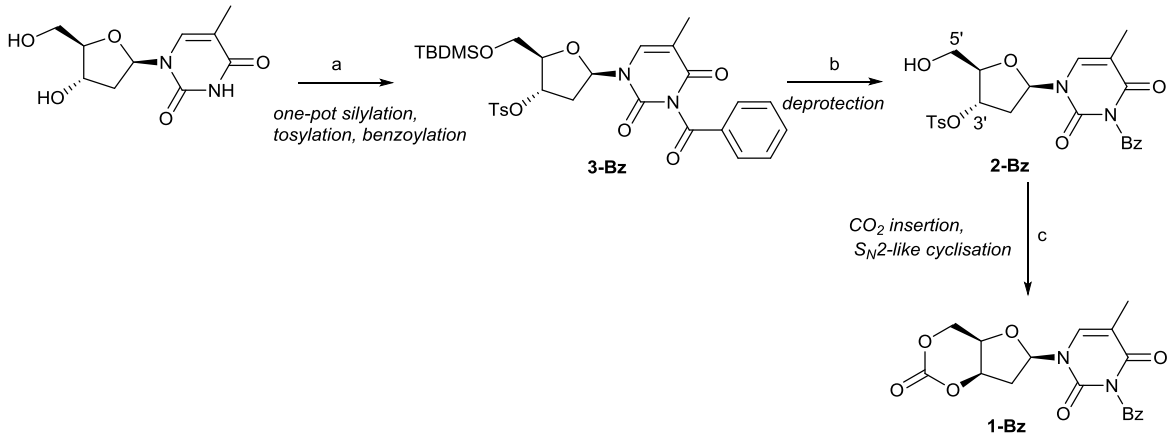

Scheme S1. Synthetic route to cyclic 3-*N*-benzoyl-3',5'-*O*-*cis*-carbonate-thymidine (**1-Bz**): (a) i): TBDMSCl, pyr, DMAP, 12 h; ii: TsCl, 24 h; iii: BzCl, 12 h; (b) 1 wt% I_2 in MeOH, reflux, 2 h; (c) DBU, CO_2, MeCN, 0- 40 °C, 24 h.

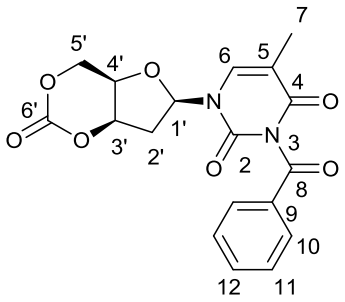

Following the procedure outlined above for the sequential one-pot silylation, tosylation of thymidine (6.00 g, 24.8 mmol, 1 equiv.), benzoyl chloride (4.30 ml, 27.2 mmol, 1.1 equiv.) was added dropwise and the reaction left to stir for a further 24 h at room temperature. Quenching with methanol and removal of volatiles *in vacuo* gave the crude 3-*N*-benzoyl-3'-TBDMS-5'-tosyl thymidine as an oily residue. This was subjected to the same deprotection and cyclisation procedures as above. Column chromatography (10% acetone/$CHCl_3$) and precipitation from dry THF gave the product as white florets (3.0 g, 33%). **R_f** 0.72 (1:1 acetone: $CHCl_3$); **Found:** C, 58.12; H, 4.41; N, 7.29. $C_{18}H_{16}N_2O_7$ requires C, 58.07; H 4.33; N 7.52%. **δ_H (400 MHz, CD_3CN)** 7.97 (2 H, dd, *J* 8.5, 1.2, H-10), 7.74 (1 H, ddd, *J* 7.2, 4.2, 1.2, H-12), 7.57 (2 H, ddd, *J* 8.5, 7.2, 1.2, H-11), 7.40 (1 H, d, *J* 1.2, H-6), 6.21 (1 H, dd, *J* 8.2, 3.6, H-1'), 5.18 (1 H, ddd, *J* 5.6, 3.8, 3.6, H-3'), 4.64 (1 H, dd, *J* 12.9, 2.2, H-5'), 4.59 (1 H, dd, *J* 12.9, 1.7, H-5'), 4.39 (1 H,

ddd, *J* 3.8, 2.2, 1.7, H-4'), 2.88 (1 H, ddd, *J* 15.9, 8.2, 5.6, H-2'), 2.44 (1 H, dd, *J* 15.9, 3.6, H-2'), 1.88 (3 H, d, *J* 1.2, 7-Me); **δ_C (101 MHz, CD_3CN)** 170.6 (C-8), 163.8 (C-4), 150.6 (C-2), 148.3 (C-6'), 136.4, 136.4 (C-6, C-12), 132.6 (C-9), 131.3 (C-10), 130.4 (C-11), 112.0 (C-5), 85.6 (C-1'), 80.9 (C-3'), 73.4 (C-4'), 67.9 (C-5'), 40.0 (C-2'), 12.7 (C7-Me); **HR-MS (ESI)** $[C_{18}H_{16}N_2O_7 + Na]^+$ Theo. 395.0855 found 395.0851. **FTIR** (thin film) cm^{-1} 1744, 1699, 1643, 1599 (C=O, C=C); **Mpt.** 163-164 °C.

1.4 General Polymerisation Procedure

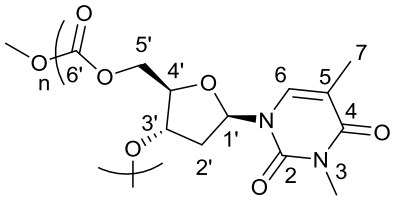

To monomer **1** (141 mg, 0.5 mmol, 100 equiv.) in anhydrous CH_2Cl_2 (0.2 ml, 2.5 M) was added 4-MeBnOH (5 µL, 1 M in CH_2Cl_2, 0.005 mmol, 1 equiv.) followed by TBD (5 µL, 1 M in CH_2Cl_2, 0.005 mmol, 1 equiv.). The mixture was stirred and monitored by ^{1}H NMR spectroscopy of aliquots taken and quenched with benzoic acid. The polymerisation was quenched by addition of a solution of excess benzoic acid (~30 equiv.) in acetone and the solvent removed under reduced pressure. The crude solid was then dissolved in CH_2Cl_2, precipitated from acetone and washed several times with acetone to removed unreacted monomer. The polymer was isolated as a white powder (80 mg, 57%). **δ_H (400 MHz, $CDCl_3$)** 7.34 (1 H, H-6), 6.25 (1 H, s, H-1'), 5.38 – 4.91 (1 H, m, H-3'), 4.30 (3 H, m, 2×H-5', H-4'), 3.28 (3 H, s, 3-*N*-Me), 2.82 (1 H, s, H-2'), 2.22 (1 H, s, H-2'), 1.92 (3 H, s, 7-Me); **δ_C (101 MHz, $CDCl_3$)** 163.4 (C-4), 154.4, 153.6, 152.8 (C=O, polycarbonate), 151.1 (C-2), 133.0 (C-6), 110.1 (C-5), 84.7 (C-1'), 79.5 (C-4'), 76.5 (C-3'), 65.4 (C-5'), 39.2 (C-2'), 27.9 (3-Me), 13.5 (7-Me). **FTIR** (thin film) 1752, 1698, 1668, 1633 cm^{-1} (C=O, C=C); ***M*$_n$ (SEC)** 15 400 g mol^{-1}, Đ 1.28; **DSC under Ar**: T_g = 155.6 °C (cooling curve of first heating cycle); **TGA under Ar:** 169- 302 °C (91% mass loss), T_{inf} = 246 °C. The polymer was insoluble in THF, EtOH, acetone, toluene, water and the PBS buffer solution used in the cell studies. It was highly soluble in chlorinated solvents namely $CHCl_3$, CH_2Cl_2 and HFIP.

L1ZnOEt was prepared according to the procedure detailed by Williams *et al.*[15] and (BDI-1)ZnEt according to Coates and co-workers.[6-7]

The same polymerisation procedure was followed for monomer **1-Bz**. The polymer was isolated as a white powder by precipitation from ether (68%). δ_H (400 MHz, $CDCl_3$) 7.91 (2 H, s, H-10), 7.64 (1 H, s, H-11), 7.49 (2 H, s, H-12), 7.33 (1 H, s, H-6), 6.42 – 5.92 (1 H, m, H-1'), 5.23 (1 H, m, H-3'), 4.86 – 3.99 (3 H, m, H-4', 2× H-5'), 2.85 (1 H, s, H-2'), 2.29 (1 H, s, H-2'), 1.97 (3 H, s, 7-Me).; **δ_C (101 MHz, $CDCl_3$)** 168.9 (C-8), 162.8 (C-4), 155.5, 154.5, 153.9 (C=O polycarbonate), 151.5 (C-2), 137.5 (C-12), 135.2 (C-6), 131.7 (C-9), 129.7 (C-10), 128.1 (C-11), 110.9 (C-5), 85.8 (C-1'), 81.6 (C-4'), 69.9 (C-3'), 65.9 (C-5'), 40.8 (C-2'), 12.8 (7-Me); ***M*n (SEC)** 11 600 g mol^{-1}, Đ 1.33; **FTIR**; 1750, 1700, 1652, 1600 (C=O, C=C).

2. NMR Spectra

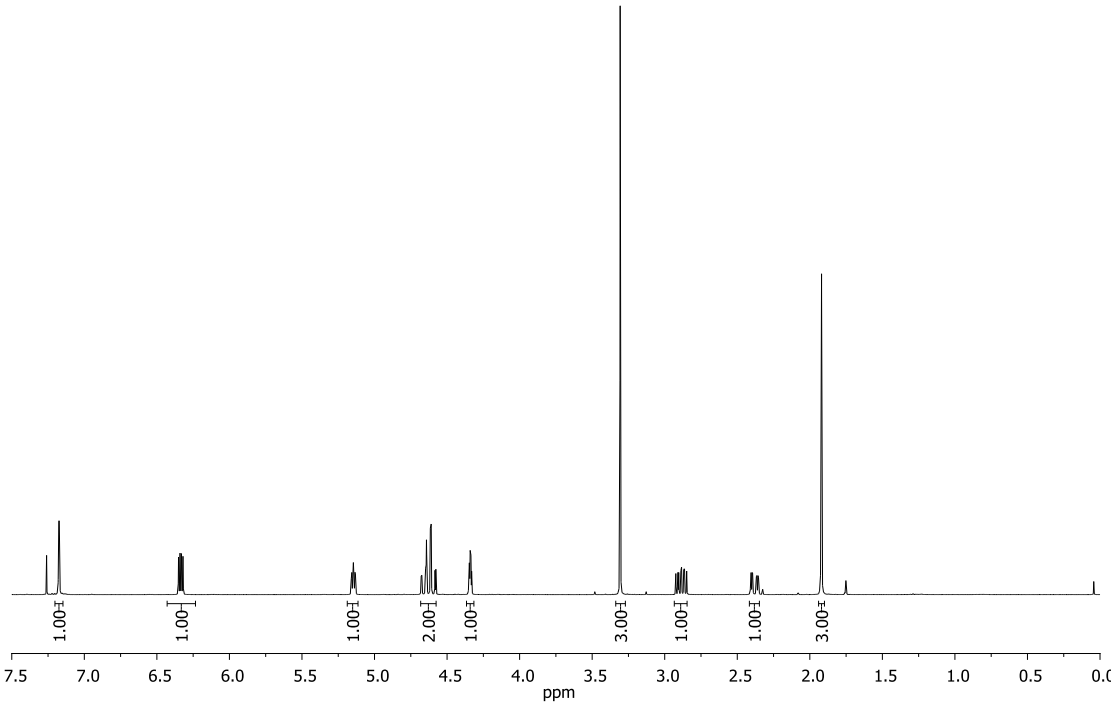

Figure S1: ^{1}H NMR Spectrum (400 MHz, $CDCl_3$) of monomer **1**.

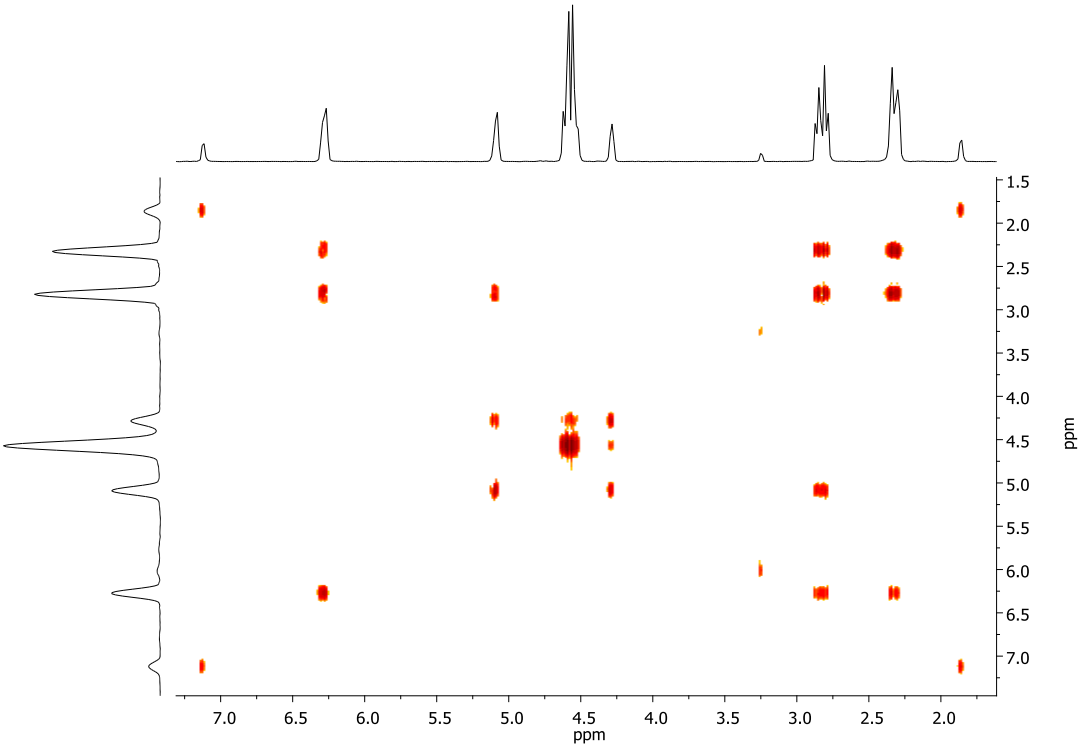

Figure S2: COSY Spectrum (400 MHz, $CDCl_3$) of monomer **1**.

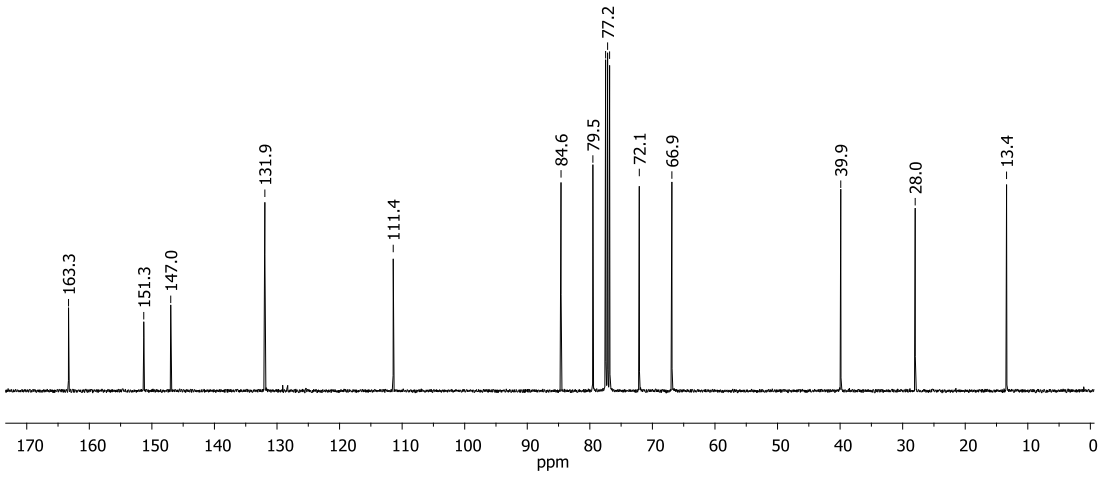

Figure S3: $^{13}C\{^1H\}$ NMR Spectrum (101 MHz, $CDC1_3$) of monomer **1**.

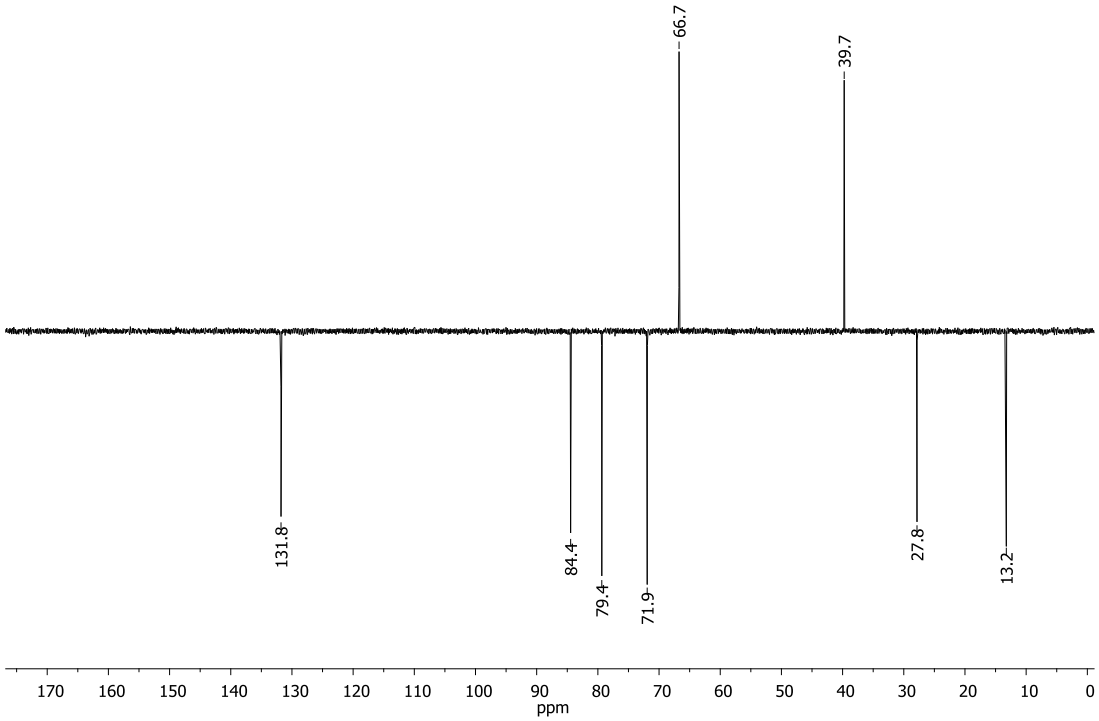

Figure S4: DEPT135 of monomer **1** in $CDCl_3$.

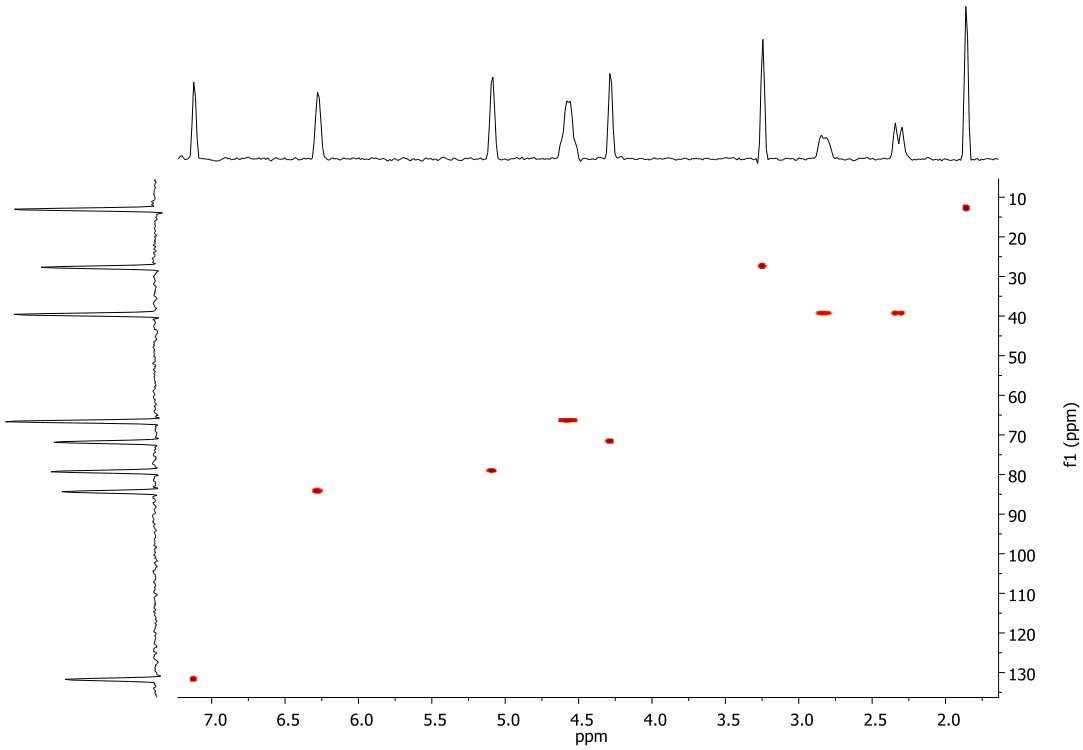

Figure S5: HSQC of monomer **1** in $CDCl_3$.

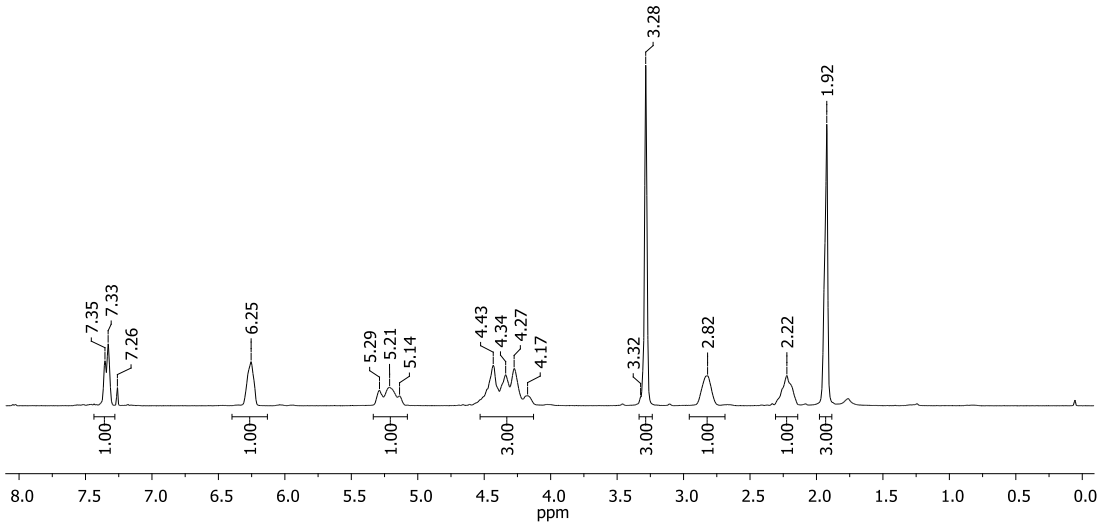

Figure S6: ^{1}H NMR Spectrum (400 MHz, $CDCl_3$) of the polymer (15 400 g mol^{-1}, Đ 1.28, Table 1, Entry 6 in article).

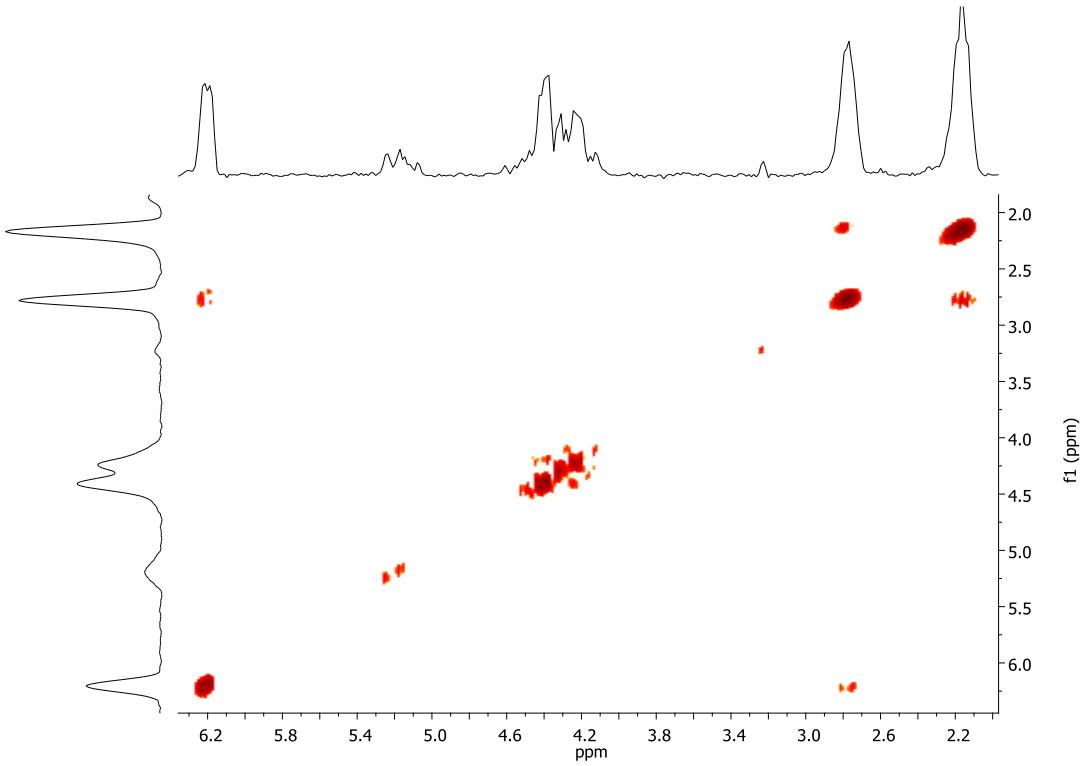

Figure S7: COSY of polymer (15 400 g mol^{-1}, Đ 1.28, Table 1, Entry 6 in article) in $CDCl_3$.

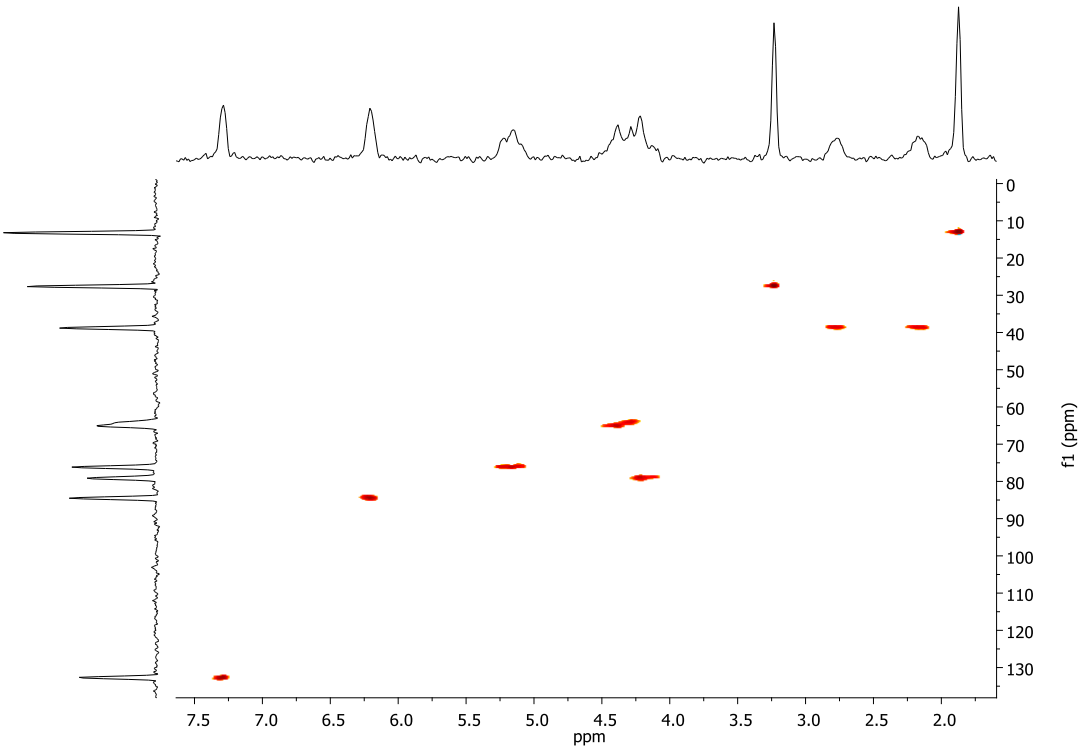

Figure S8. HSQC of polymer (15 400 g mol^{-1}, Đ 1.28, Table 1, Entry 6 in article) in $CDCl_3$.

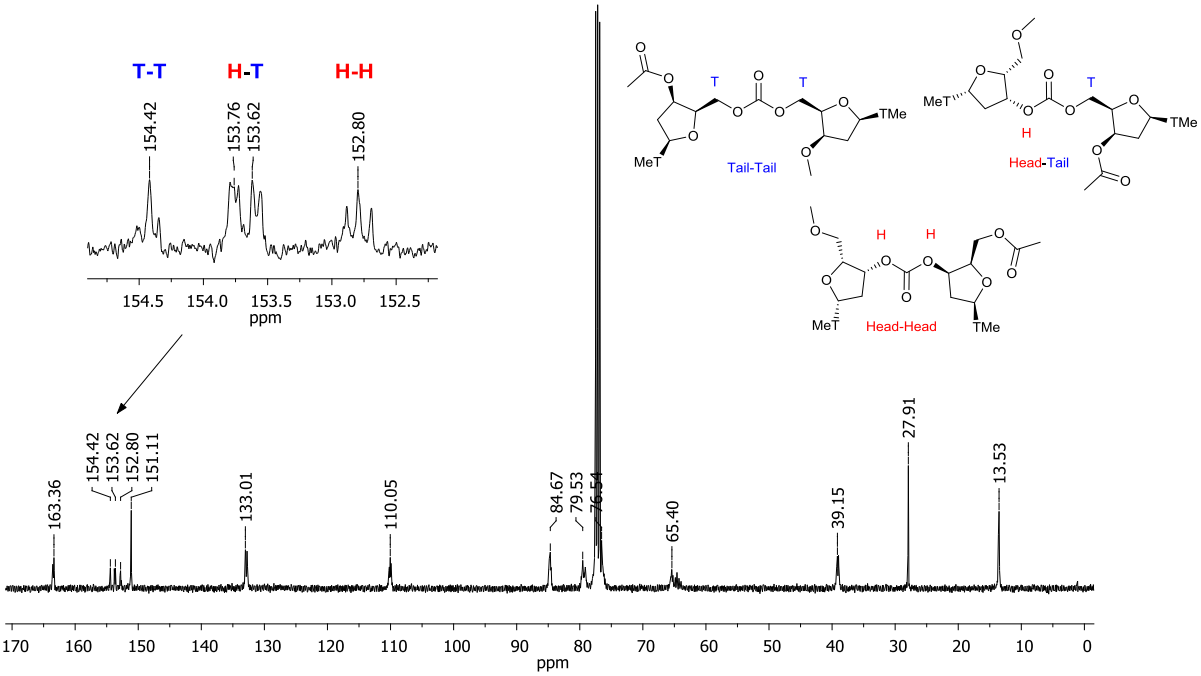

Figure S9. $^{13}C\{^1H\}$ NMR Spectra (400 MHz, $CDCl_3$) of polymer (15 400 g mol^{-1}, Đ 1.28, Table 1, Entry 6 in article).

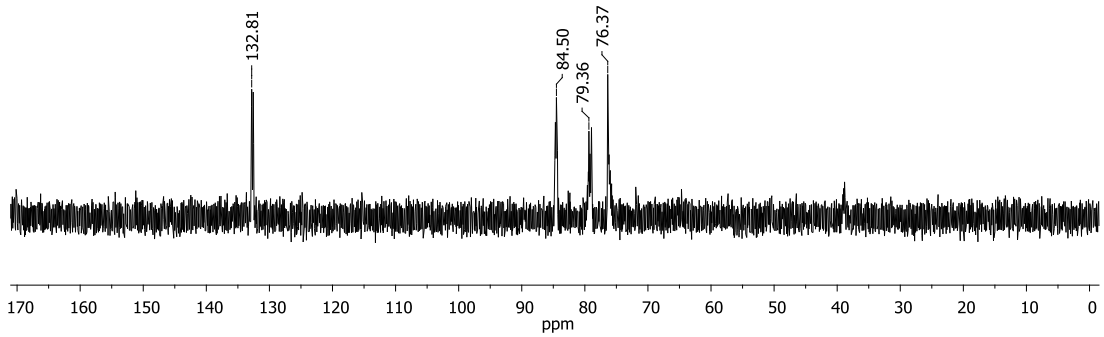

Figure S10. DEPT90 of polymer (15 400 g mol^{-1}, Đ 1.28, Table 1, Entry 6 in article) in $CDCl_3$.

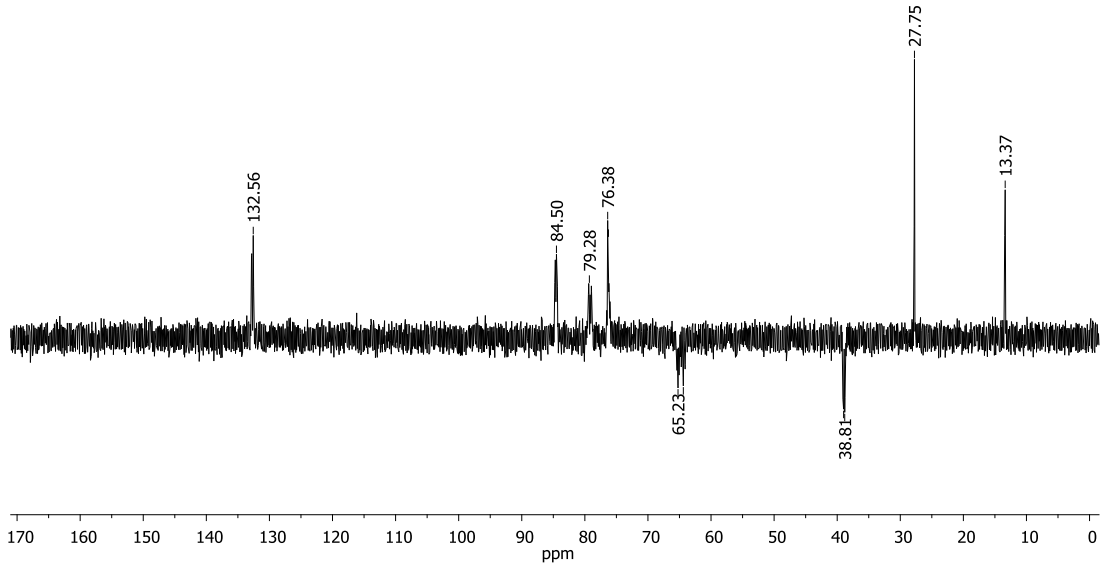

Figure S11. DEPT135 of polymer (15 400 g mol^{-1}, 1.28 Đ, Table 1, Entry 6 in article) in $CDCl_3$.

Cyclic 3-N-benzoyl- 3',5'-O-cis-carbonate-thymidine (1-Bz)

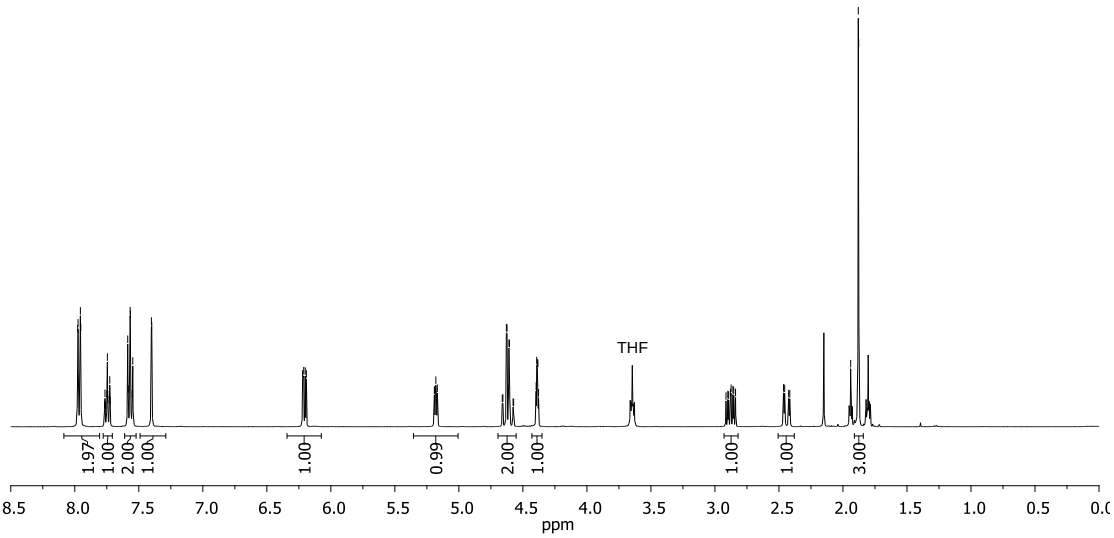

Figure S12. ^{1}H NMR spectrum (400 MHz, MeCN-d_3) of **1-Bz**.

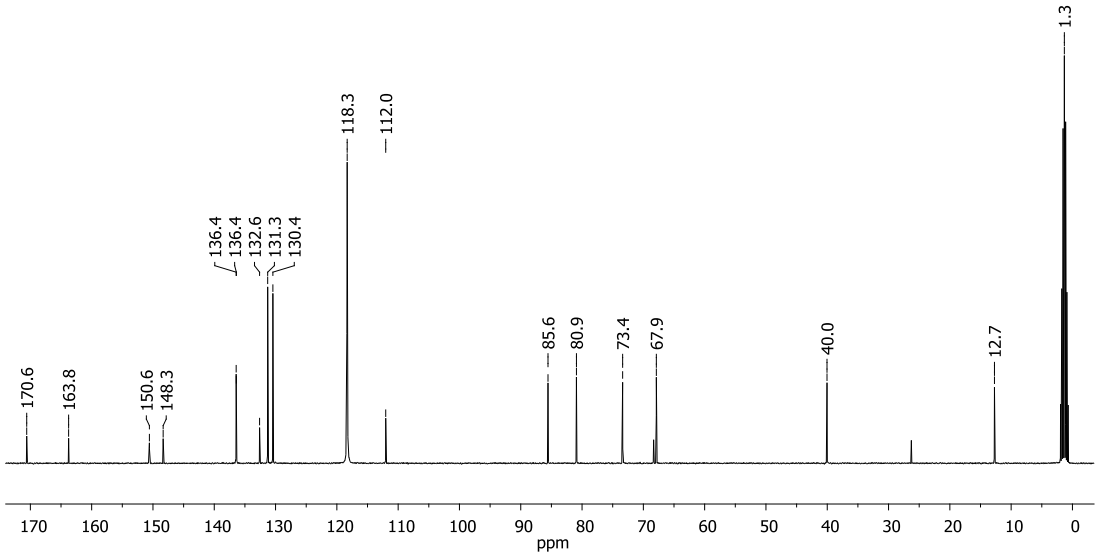

Figure S13. $^{13}C\{^{1}H\}$ NMR spectrum (101 MHz, MeCN-d_3) of **1-Bz**.

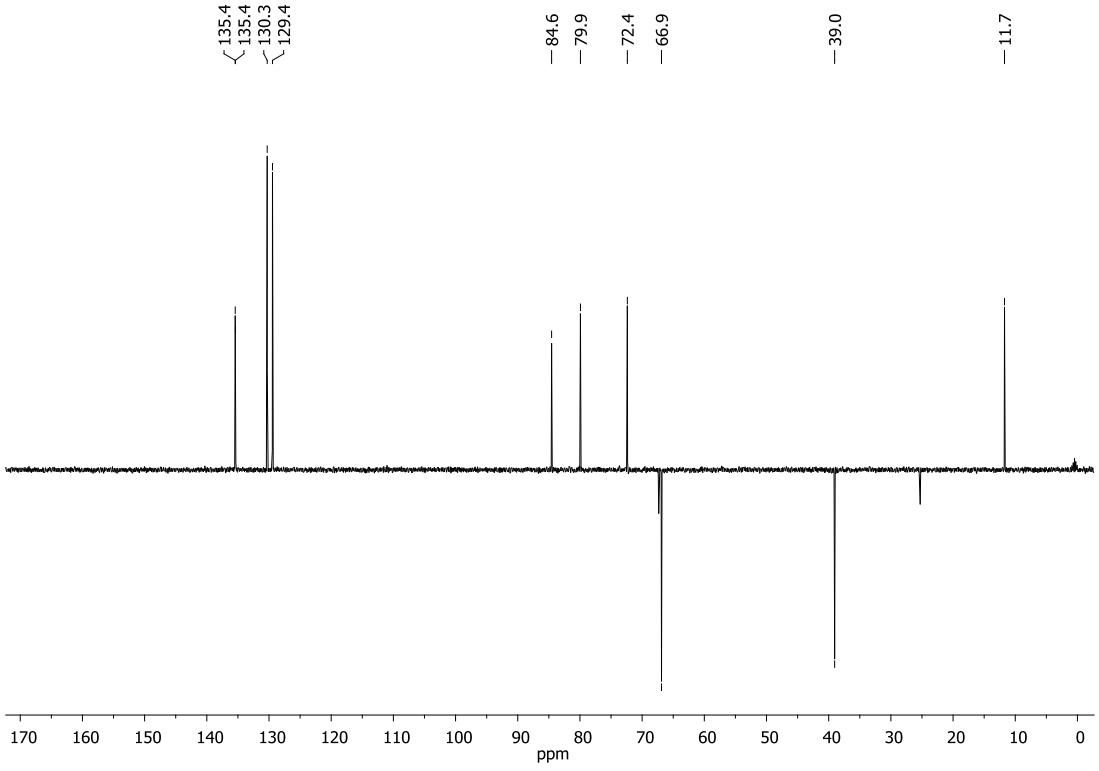

Figure S14. DEPT135 of **1-Bz** in MeCN-d_3.

3. Kinetic Experiments

Kinetic experiments were carried out by taking aliquots of the polymerisation mixture at specific time intervals and quenching with excess benzoic acid in $CDCl_3$.

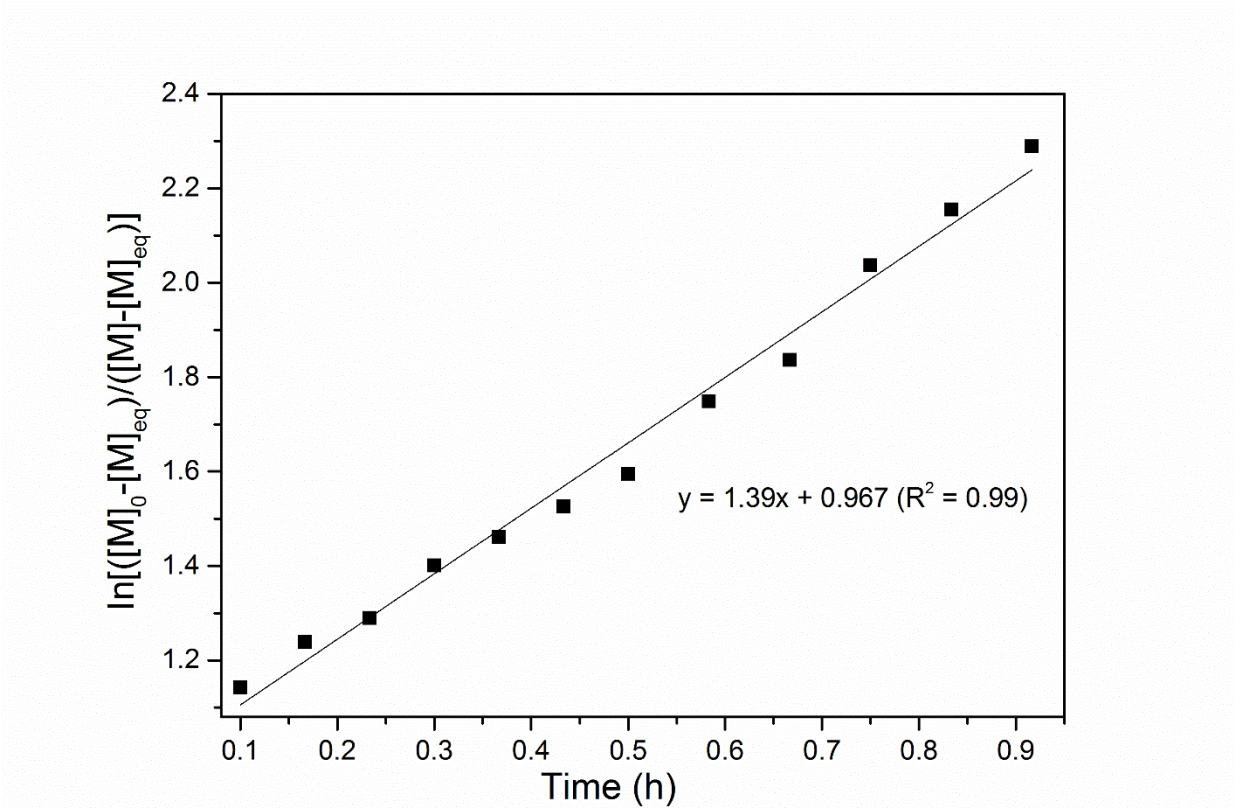

Figure S15. Kinetic plot for equilibrium polymerisation of **1** with 4-MeBnOH and TBD catalyst carried out under the following conditions: $[M]_0$= 0.5 mol L^{-1} in CH_2Cl_2, 100:1:1 $[\mathbf{1}]_0$: $[4\text{-MeBnOH}]_0$: $[TBD]_0$ and 25 °C. An equilibrium monomer conversion $[M]_{eq}$ = 0.16 mol L^{-1} was used giving an apparent pseudo-first order rate constant k_{app} = 1.39 ± 0.005 h^{-1} (linear fit, R^2 =99%). Off-set from 0,0 due to monomer not being completely soluble in the CH_2Cl_2 solvent at these conditions.

4. Size-Exclusion Chromatography

Molecular Weight Averages

Peak	Mp	Mn	Mw	Mz	Mz+1	Mv	PD
Peak 1	8656	7654	8347	8994	9600	8902	1.091

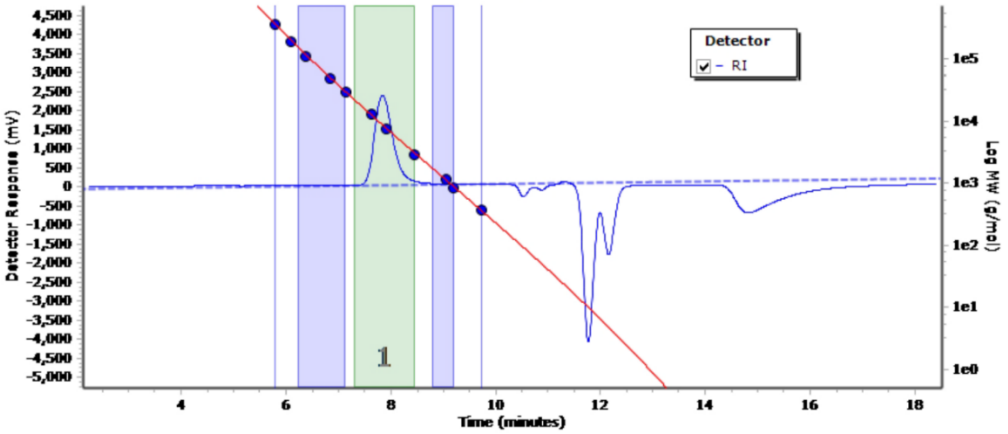

Figure S16. SEC trace of polymer showing M_n 7650 g mol^{-1}, Đ 1.09 (data point 7, Figure 6 in article).

Molecular Weight Averages

Peak	Mp	Mn	Mw	Mz	Mz+1	Mv	PD
Peak 1	8550	7214	8069	8779	9386	8684	1.119

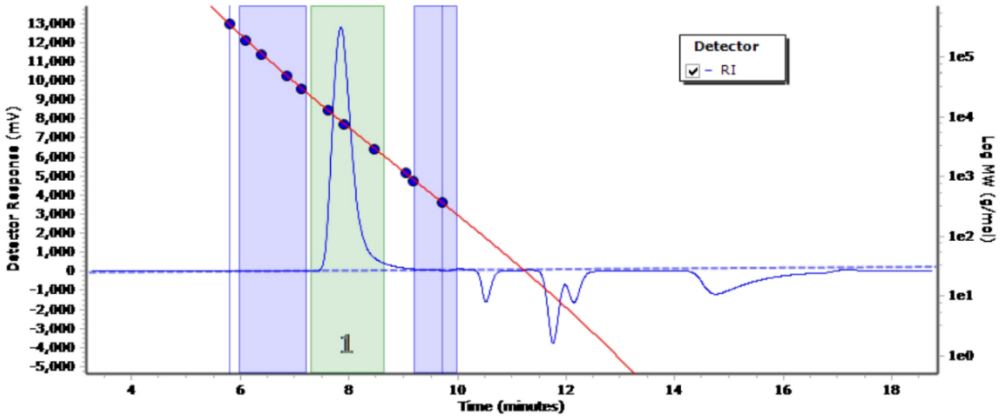

Figure S17. SEC trace of polymer showing M_n 7210 g mol^{-1}, Đ 1.12 (Figure 7 in article).

Molecular Weight Averages

Peak	Mp	Mn	Mw	Mz	Mz+1	Mv	PD
Peak 1	22097	15445	19834	24282	28272	23663	1.284

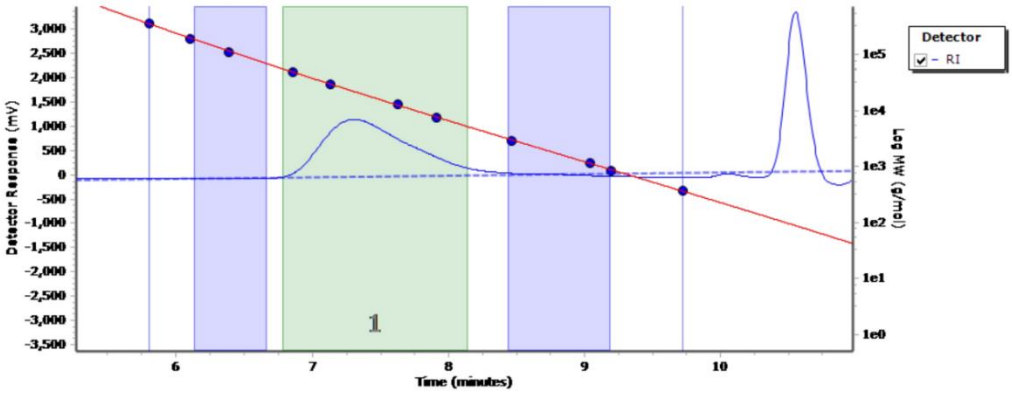

Figure S18. SEC trace of polymer showing M_n 15 400 g mol^{-1}, Đ 1.28 (Table 1, Entry 6 in article).

5. End-group Analysis by MALDI-ToF Mass Spectrometry

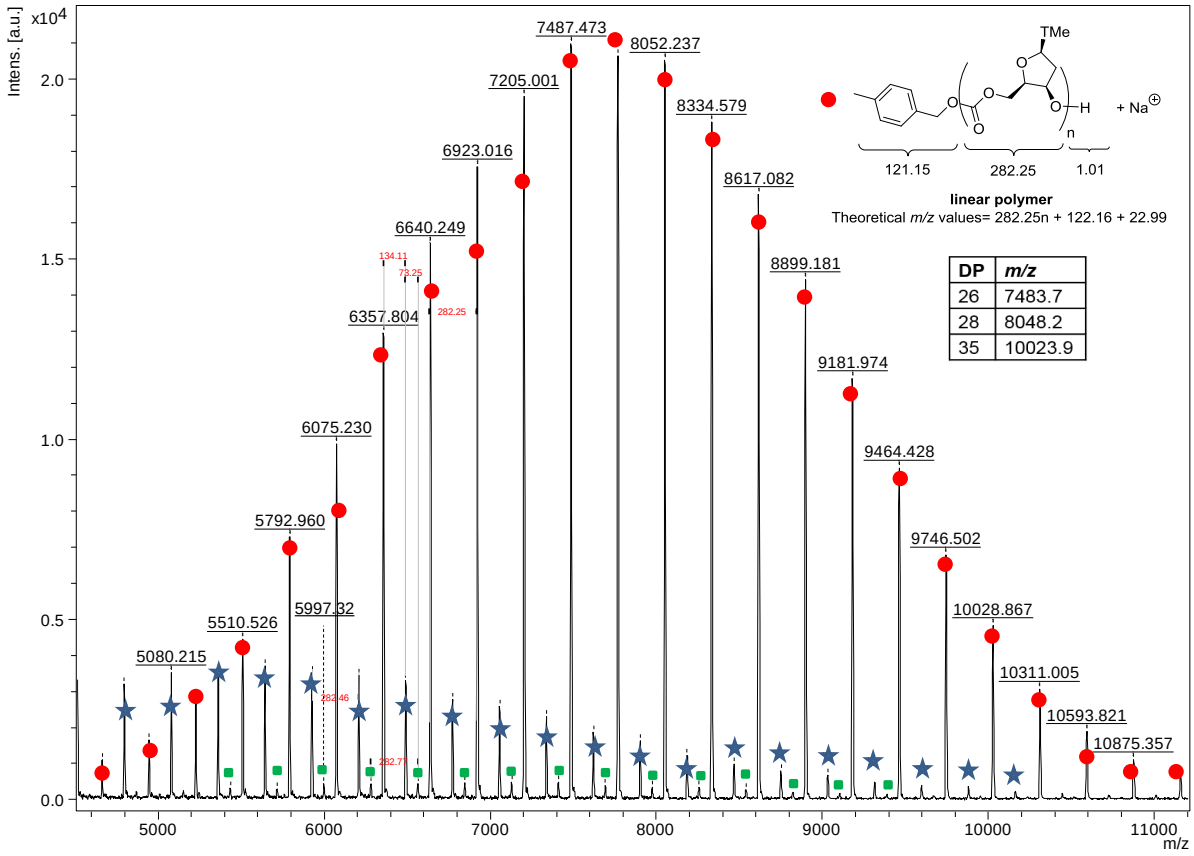

Figure S19. MALDI-ToF MS of polymer ($M_{n,sec}$ 7210 g mol^{-1}, Đ 1.12, Figure 7 in article). Major series (81 %, red circle) corresponds to sodium adduct of linear polymer with OH and 4-methylbenzyl alcohol end-groups ($M_{n,\,MALDI}$ 7120 g mol^{-1}, Đ 1.03). Minor series (19%, blue star) with same repeat unit ~282.25 *m/z* corresponds to proton adduct of cyclic species ($M_{n,\,MALDI}$ 5250 g mol^{-1}, Đ 1.01), for example DP=18 gives *m/z* 282.25x18+1.01 = 5081.51). Very minor series (green square) with same repeat unit ~282.25 *m/z* corresponds to proton adduct of linear polymer with OH and trifluoroacetate Methymidine end groups, presumably from the break-down of cyclic species and decarboxylation by trifluoroacetate anions used in the matrix. For example DP=20 gives *m/z* 113.99 + 238.26 + 20*282.25 +1.01 = 5998.17).

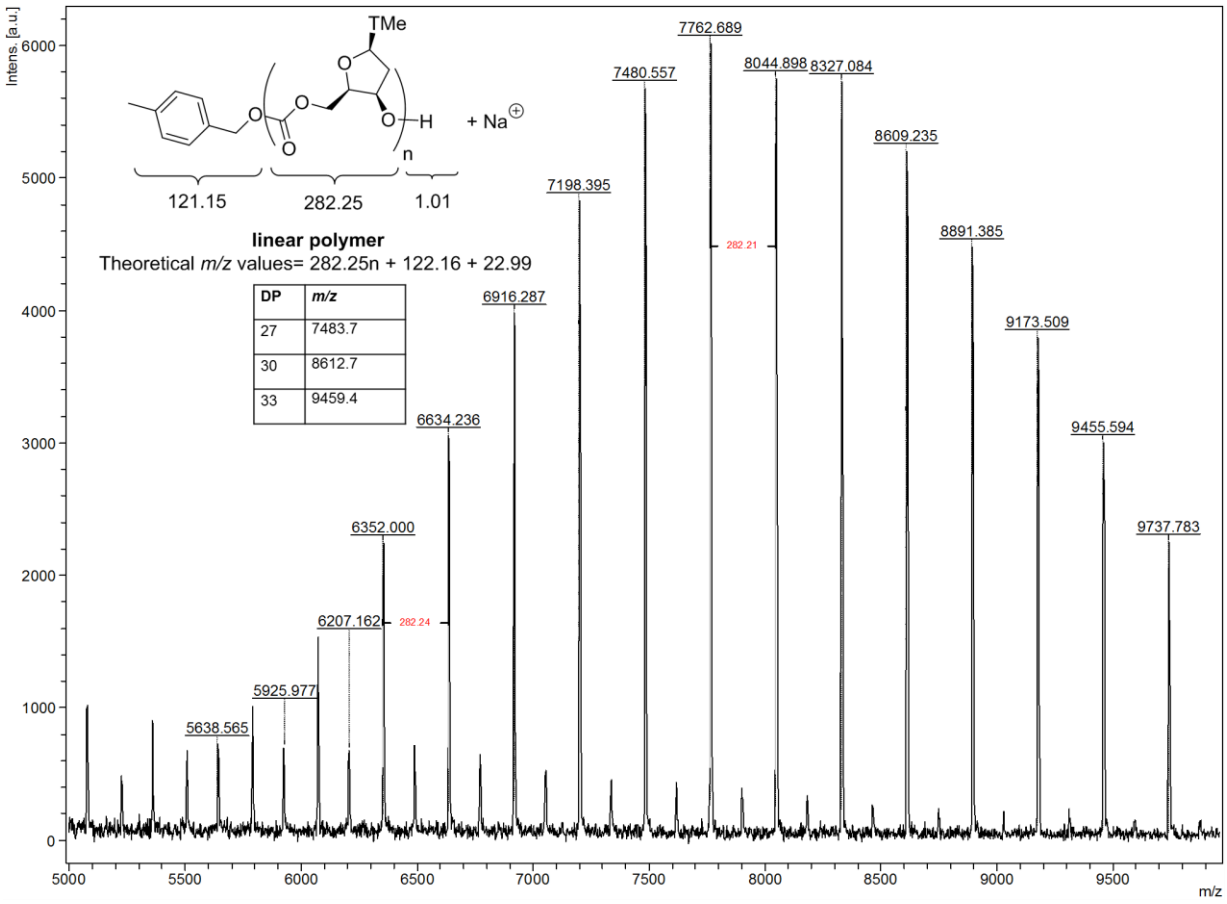

Figure S20. Further example of MALDI-ToF analysis of polymer ($M_{n,sec}$ 7660 g mol^{-1}, Đ 1.19) showing sodium adduct of linear polymer with OH and 4-methylbenzyl alcohol end-groups ($M_{n,\,MALDI}$ 7650 g mol^{-1}) as major series.

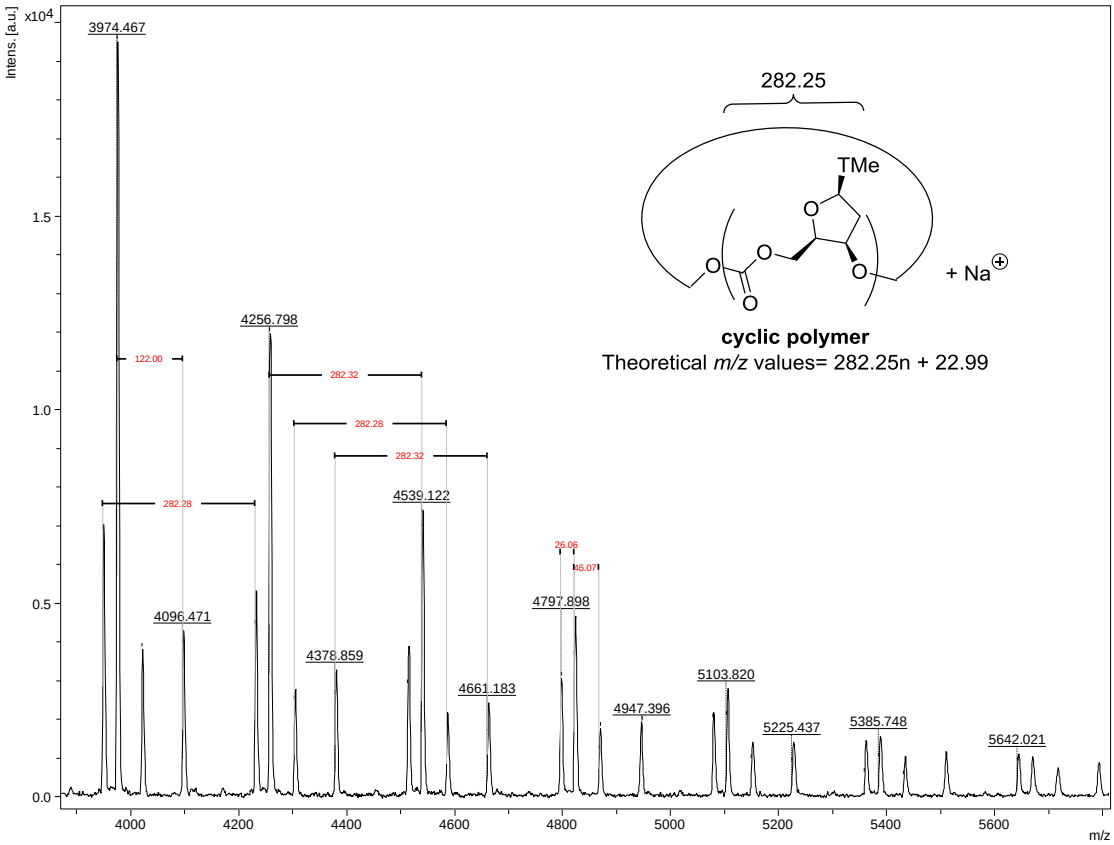

Figure S21. MALDI-ToF analysis of polymer ($M_{n,sec}$ 4260 g mol^{-1}, Đ 1.09, Table 1, Entry 1 in article) obtained under higher dilution conditions ($[M]_0$ = 0.5 mol L^{-1}) showing the cyclic polymeric species (P_c) as the major series; $[P_c + Na]^+$ (DP=15 gives *m/z* 4256.7) and $[P_c + H]^+$ (DP= 17, *m/z* 4798.3). The minor series corresponds to the linear polymer $[P_L + Na]^+$ (DP=14 gives *m/z* 4096.7).

6. Polymer Thermal Properties

6.1 TGA-MS

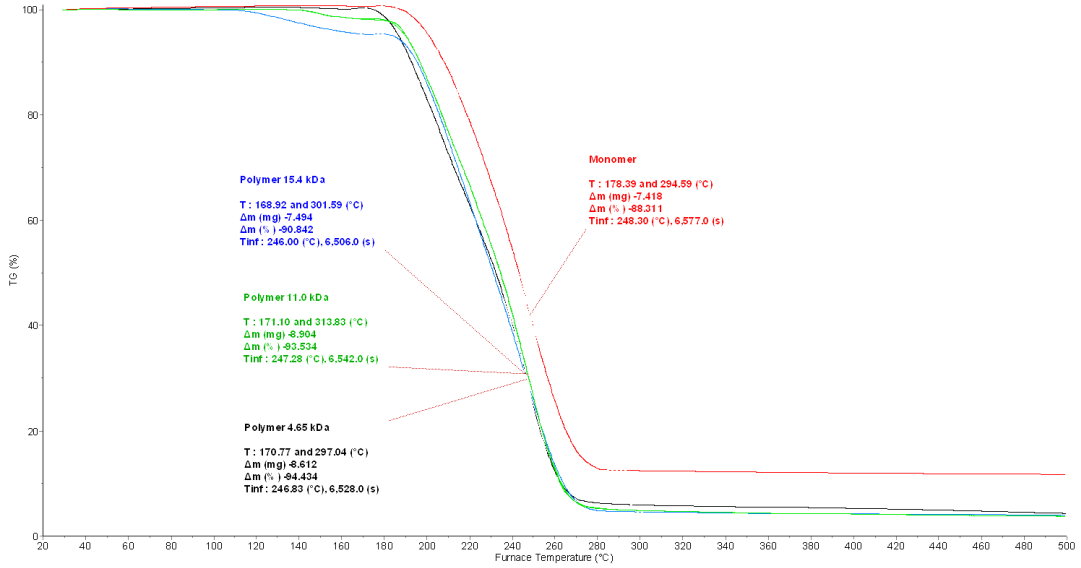

Figure S22. TGA analysis of polymers of different M_n (Table 1, Entries 5 and 6) and monomer **1** for comparison.

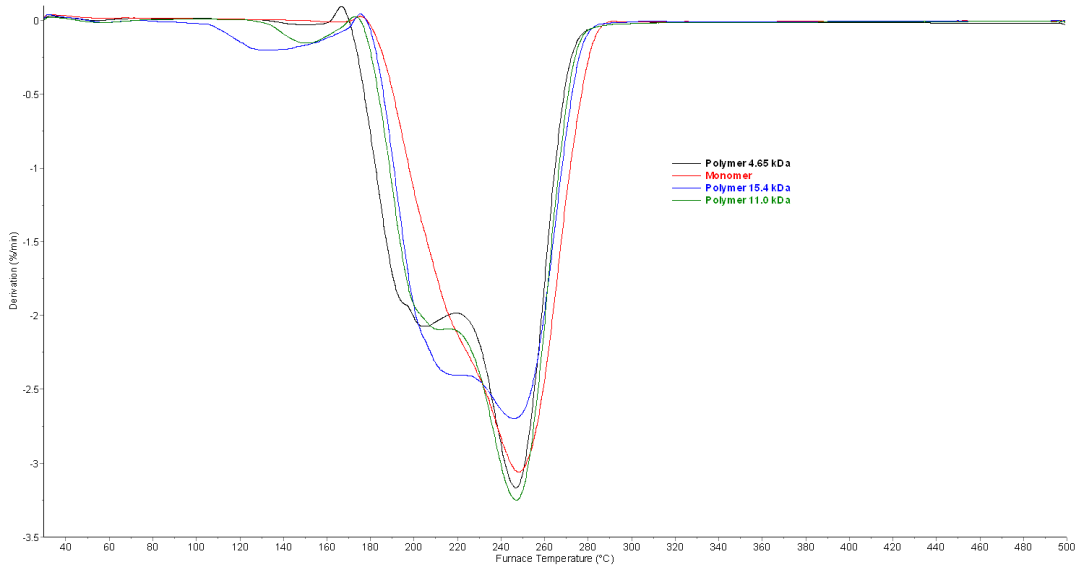

Figure S23. Derivative of TG curves shown above. Two events appear to occur in the decomposition of the polymers.

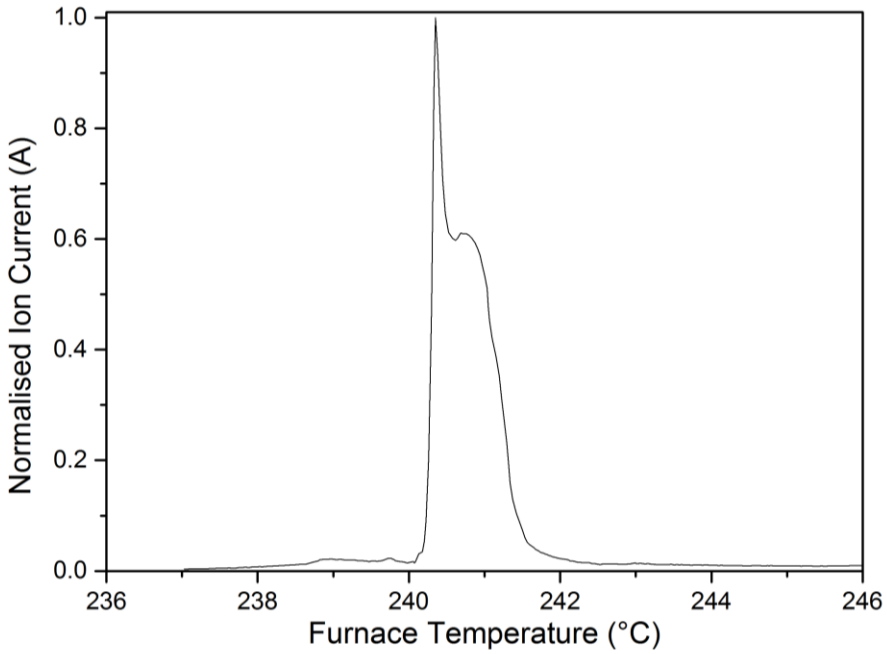

Figure S24. Normalised ion current as a function of furanace temperature (°C) for *m/z* 44 assigned to CO_2^+ during the decomposition of polymer (M_n 15 400 g mol^{-1}, Đ 1.28, Table 1, Entry 6 in article).

6.2 DSC Traces

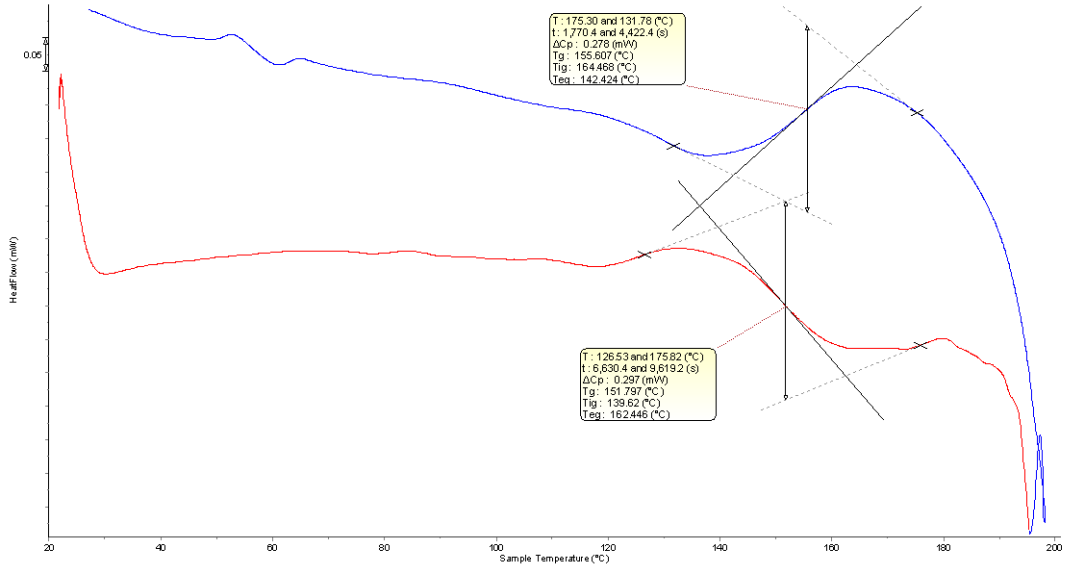

Figure S25. First heating (red) and cooling (blue) cycle for polymer (15 400 g mol^{-1}, Đ 1.28, Table 1, Entry 6 in article). Exotherm up.

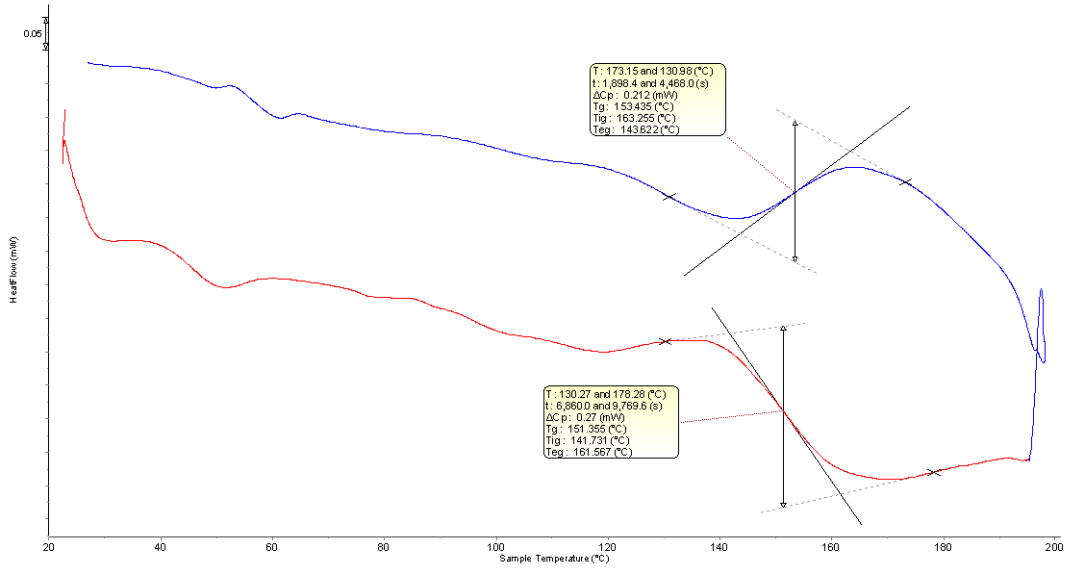

Figure S26. First heating (red) and cooling (blue) cycle for polymer (11 000 g mol^{-1}, Đ 1.27, Table 1, Entry 5 in article). Exotherm up.

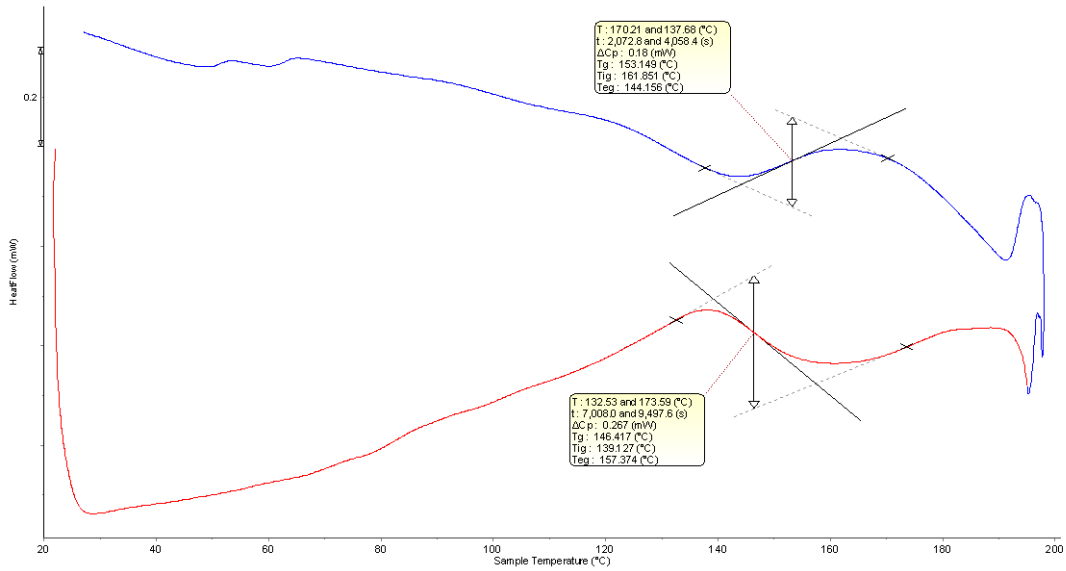

Figure S27. Second heating (red) and cooling (blue) cycle for polymer (4650 g mol^{-1}, Đ 1.09). Exotherm up.

Polymer of 1 (g mol^{-1})	**T_g (°C)**
15 400	155.6
11 000	153.4
4650	153.1

Table S1. Summary of T_g values for polymers (Figures S25-S27). Values have been taken from the cooling down cycle.

7. Powder X-ray Diffraction

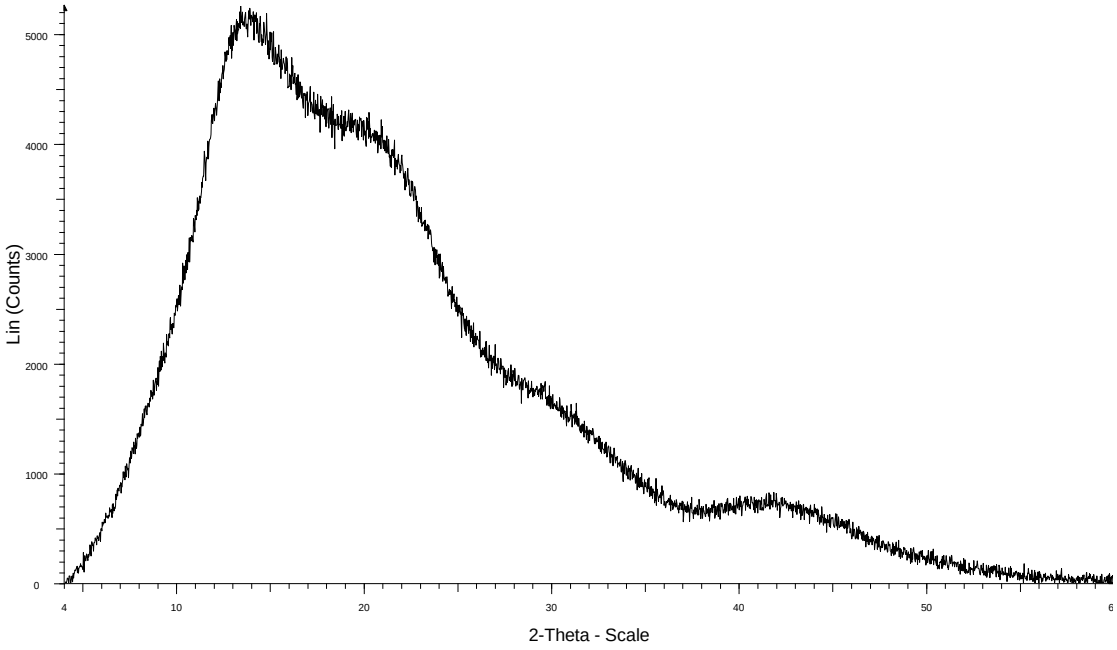

Figure S28. Powder X-ray diffraction of polymer (15 400 g mol^{-1}, Đ 1.28, Table 1, Entry 6 in article) showing amorphous character.

8. Hydrolytic Studies

The polymer was observed over several weeks not to dissolve in D_2O even at 0.25 wt% but did however dissolve in 1 M NaOH solution after 4-6 hours at 0.25 wt%. Complete hydrolytic degradation of the water insoluble polymer to release CO_2 and the free sugar diol would be expected to result in dissolution of the polymer. To confirm the water solubility of the hydrolytic degradation product, 3-*N*-methyl-thymidine was prepared according to the literature procedure[2] but found to be insoluble in water. However, monomer **1** was observed to slowly dissolve in water. NMR spectroscopy and HR-MS (ESI) confirmed ring-opening of **1** by H_2O/D_2O and subsequent decarboxylation to give the corresponding 3-*N*-methyl-3',5'-cis-thymidine diol (Figures S29 and S30). Thus, the hydrolytic degradation product of the polymer is highly water soluble.

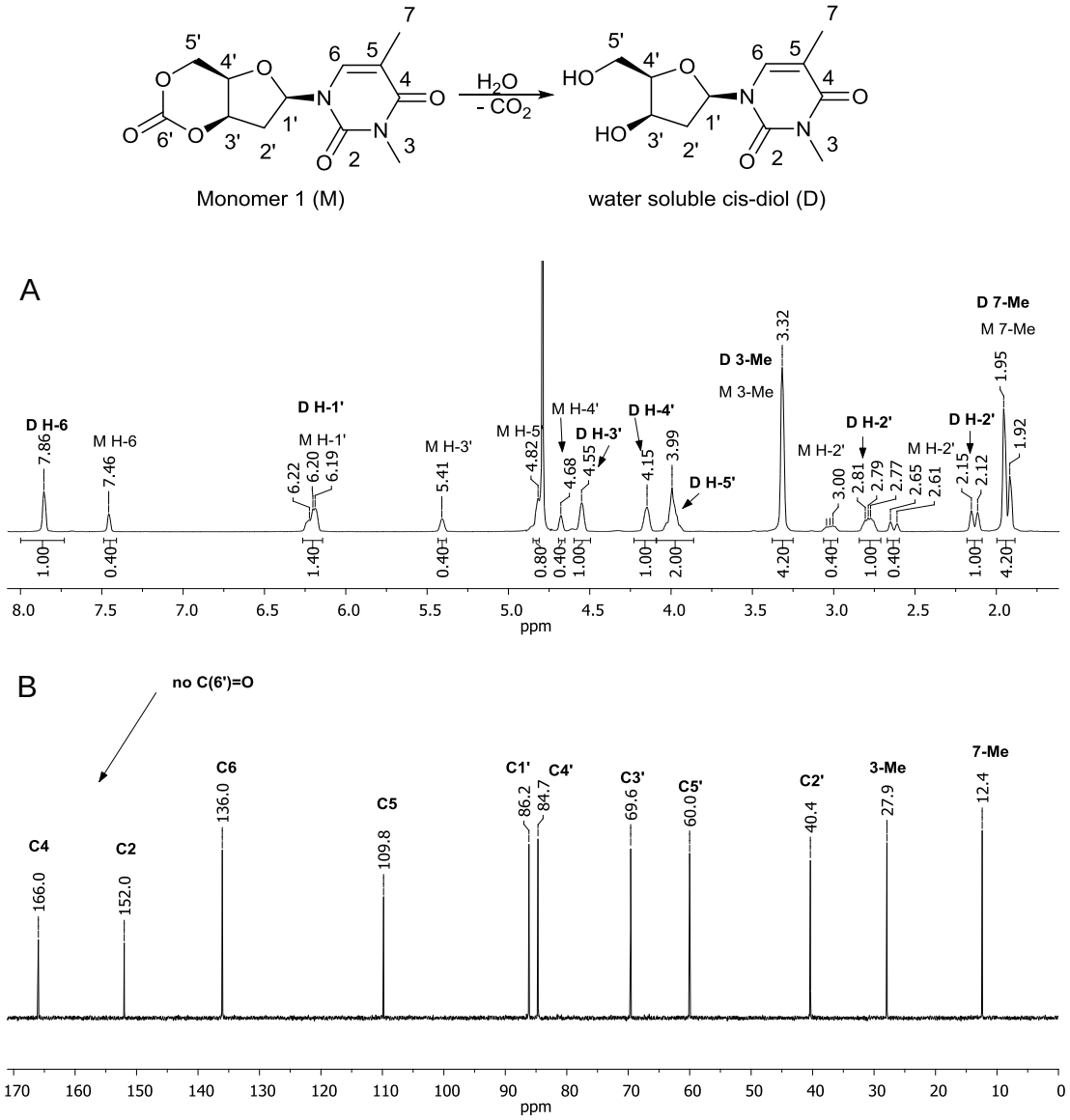

Figure S29. A: ^{1}H NMR spectrum (400 MHz, D_2O) of monomer **1** (M) showing 71% conversion after 12 h to D_2O ring-opened *cis*-diol (D). Clear changes in the H-3', H-4' and H-5' proton environments are observed between M and the ring-opened D. **B:** $^{13}C\{^{1}H\}$ NMR (101 MHz, D_2O) of fully ring-opened monomer confirming loss of C=O of cyclic carbonate. This illustrates the water-soluble nature of the *cis*-diol, the hydrolytic degradation product of the polymer. Full NMR assignment was aided by COSY, HSQC and DEPT135 NMR experiments. HR-MS (ESI) confirmed the anion of the diol $[C_{11}H_{15}N_2O_5]^-$ Theo. m/z 255 098097 found 255.0980 m/z.

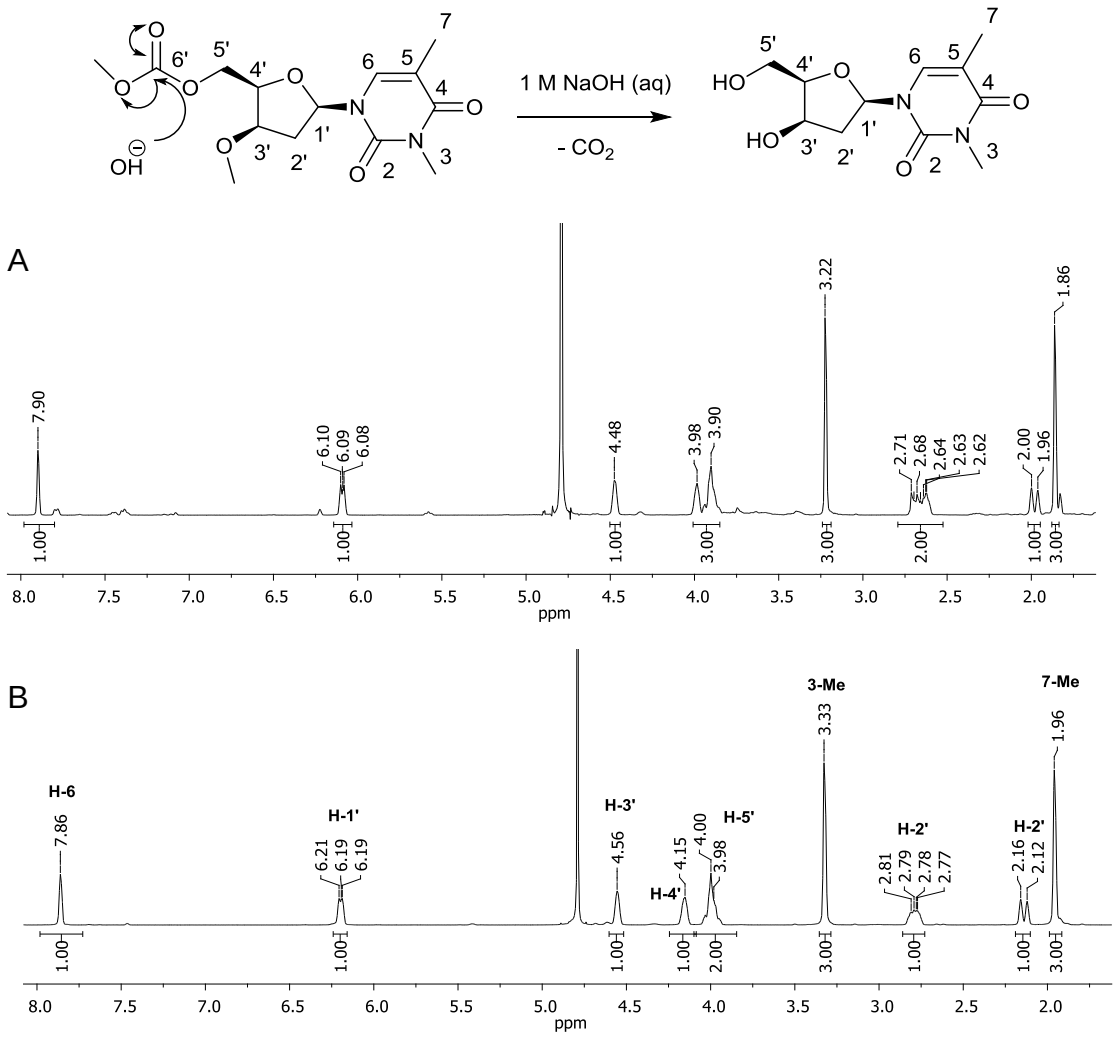

Figure S30. Comparison showing close agreement of the ^{1}H NMR spectra (400 MHz, D_2O) of **A:** the hydrolytic degradation products of the water insoluble polymer (4 wt% polymer in 1 M NaOH in D_2O) and **B:** the component *cis*-sugar diol prepared by ring-opening of monomer **1** in D_2O (>99% conversion). Full assignments were aided by COSY, DEPT135 and HSQC experiments.

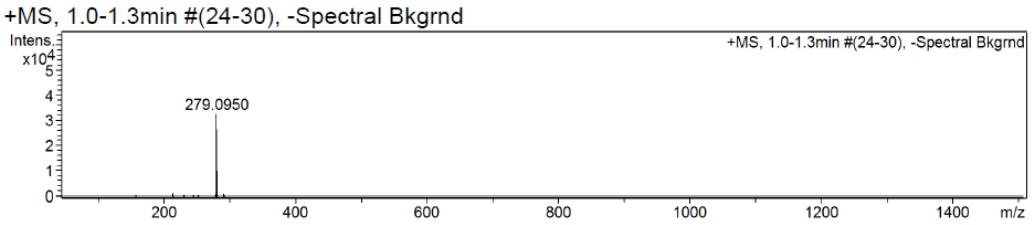

#	m/z	I	I %	Area	S/N
1	158.0269	489	1.5	6	6035.0
2	198.1832	298	0.9	7	1214.9
3	214.0876	1086	3.3	20	2105.6
4	231.1225	338	1.0	12	420.5
5	245.1348	394	1.2	16	377.3
6	253.1154	564	1.7	25	478.6
7	279.0950	32437	100.0	1604	20026.4
8	280.0986	3331	10.3	176	2035.2
9	281.1008	405	1.2	22	244.8
10	291.1991	1062	3.3	16	615.6

Figure S31. HR-MS (ESI) further confirmed the sodium adduct of the diol; $[C_{11}H_{16}N_2O_5 + Na]^+$ Theo. m/z 279.095691 found 279.0950. No dimmers or trimmers were detected. Mass spectrum recorded as soon as all polymer (5 mg) was observed to dissolve in 1 M NaOH (2 ml) ~ 4 h.

9. Contact Angle Measurements

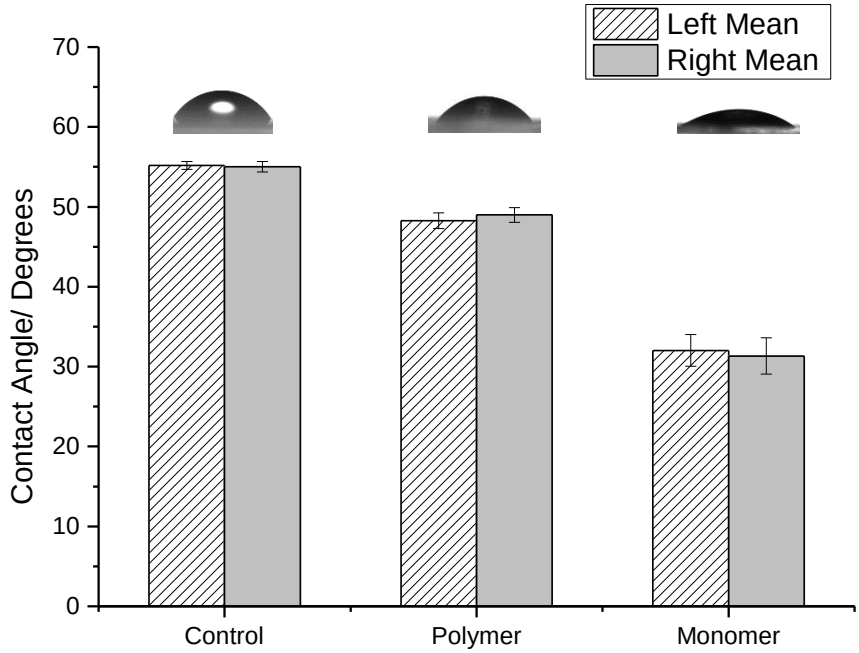

Figure S32. Right and left static water contact angle measurements for thin films of polymer drop casted onto glass slides compared to the glass cover slip as a control and thin films of the monomer prepared in the same way. Values represent an average of 10 measurements taken from three films. Error bars represent the standard error of the mean (n=10). A greater error was observed for the monomer as the films were less even due to crystal formation.

10. Cell Attachment Studies

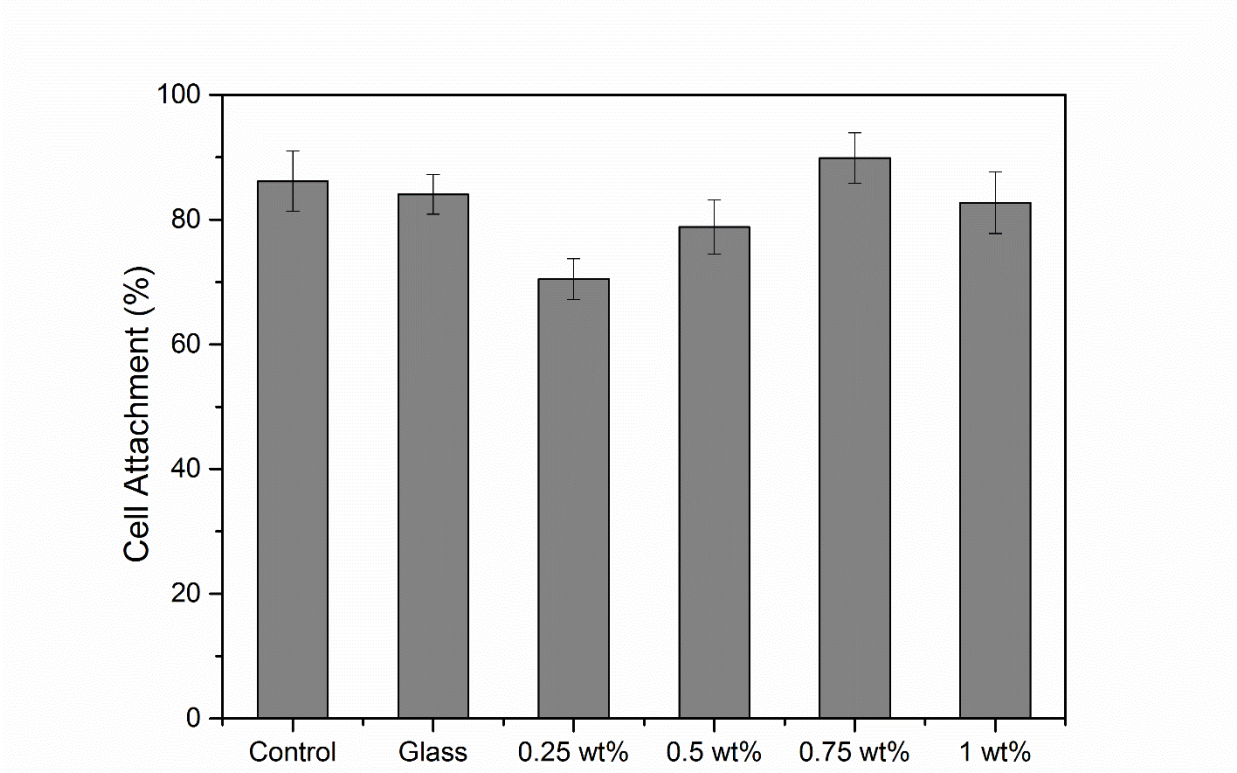

Figure S33. Number of MG-63 cells attached after a 1 h incubation period (37 °C, 5% CO_2) expressed as a percentage of the seeding density (10,000 cells cm^{-2}) for polymer thin films prepared by drop casting solutions of different wt% onto glass slides and compared to the glass slide (glass) and empty culture plate well (control). Values are reported as an average with error bars representing standard error (n=18). Variation between different wt% of polymer solutions is attributed to the quality of the film formed, drop casting often results in non-uniform films. Polymer scaffolds prepared using a heat press were found to be too brittle for cell experiments.

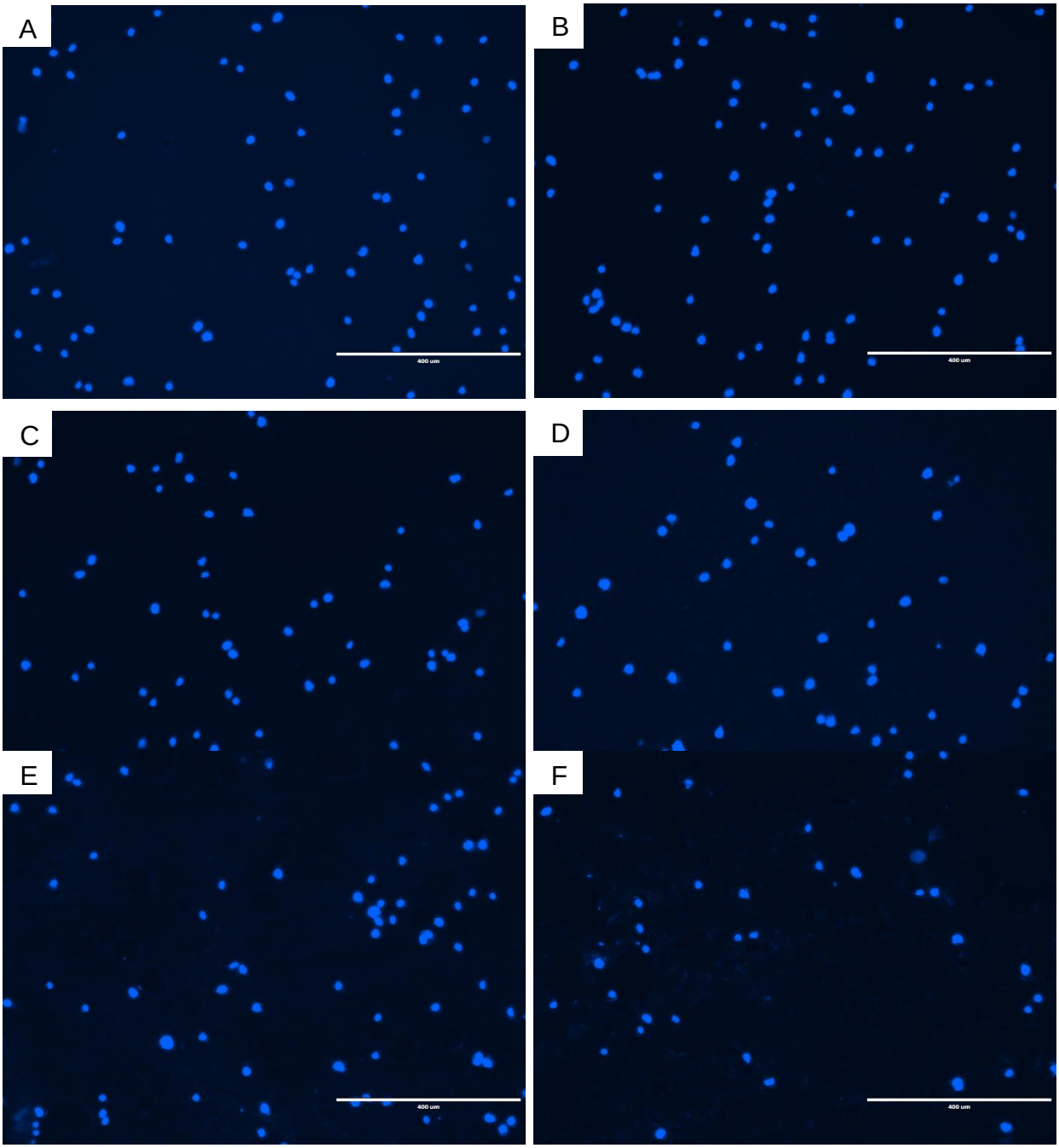

Figure S34. Confocal microscopy images of cells stained with DAPI after the 1 h incubation period for A) the empty well-plate control, B) the glass control and polymer films prepared by drop casting solutions of C) 0.25 wt%, D) 0.5 wt%, E) 0.75wt% and F) 1 wt %.

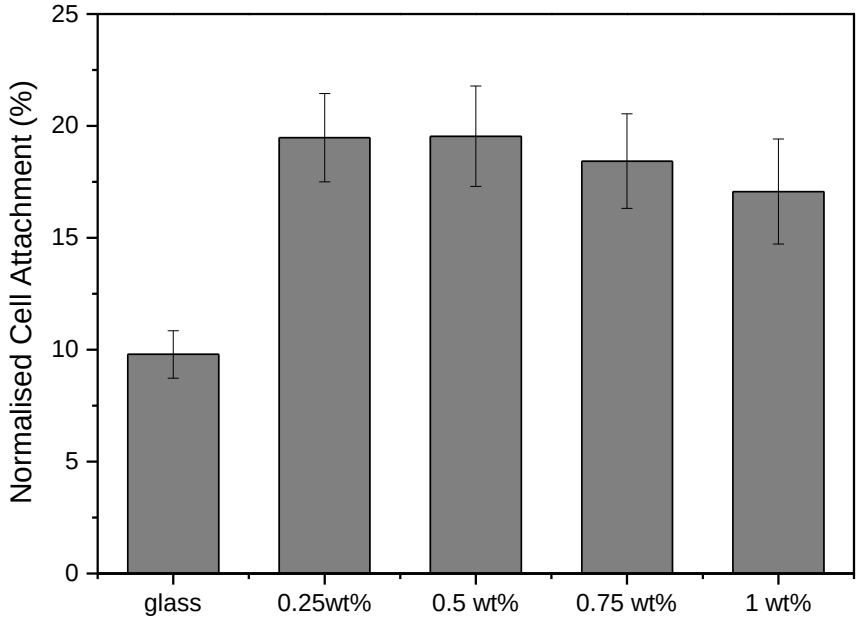

Figure S35. The number of MG-63 cells attached after a 24 h incubation period (37 °C, 5% CO_2) as a percentage of the seeding density (10,000 cells cm^{-2}) and normalised to the empty polystyrene well-plate control. Values represent mean values and error bars standard error (n=18). Statistically more cells are attached to the polymer films compared to the glass slide control, which may be a result of the roughness of the polymer film surface due to the drop casting method.

11. DFT Computational Details

All calculations were performed using the Gaussian09 suite of codes (revision D.01).[9] Geometries were fully optimised without any symmetry or geometry constraints using the rωB97XD LC hybrid functional developed by Chai and Head-Gordon. This includes an empirical dispersion correction and has been shown to effectively reproduce thermodynamic and kinetic experimental data.[3-5] Calculations were carried out using a temperature of 298K and solvent effects in acetonitrile (for ring-closing calculations) and dichloromethane (for ring-opening) considered using a conductor-like polarisable continuum model (CPCM).[8, 12, 16]

The nature of all the stationary points as minima or transition states was verified by calculations of the vibrational frequency spectrum. All transition states were characterised by precisely one imaginary mode corresponding to the intended reaction. In this study, no IRC calculations were performed to further confirm the identity of the reaction. The vibrational data were used to relax the geometry of each transition state toward reactants and products, in order to confirm its nature. However, only the most stable conformational isomers are reported for all intermediates. Free energies were calculated within the harmonic approximation for vibrational frequencies.

11.1 Ring-closing Cyclisation

Nucleophilic Addition-Elimination Pathway

At the rωb97xd/6-31+G(d)/cpcm=acetonitrile/298 K level of theory, both kinetic and thermodynamic barriers to ring-closing by nucleophilic attack of the free hydroxyl group at the tosylated carbonate are reasonable for formation of the *trans*-3',5'-cyclic carbonate of 3-*N*-methyl thymidine. For comparison, the analogous parameters at the same level of theory are calculated for reported *trans*-fused pyranose monomers derived from D-glucose and D-mannose.

***Trans*-3',5'-cyclic carbonate of 3-*N*-methyl-thymidine**

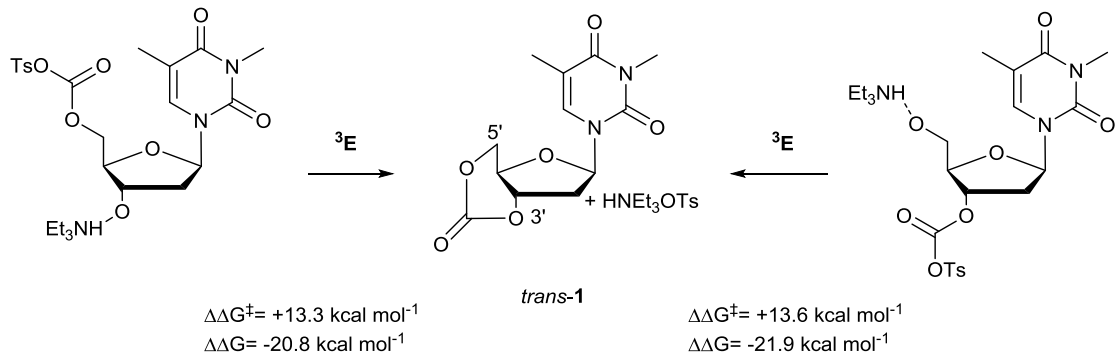

trans-**1**

$\Delta\Delta G^{\ddagger}$= +13.3 kcal mol^{-1}
$\Delta\Delta G$= -20.8 kcal mol^{-1}

$\Delta\Delta G^{\ddagger}$= +13.6 kcal mol^{-1}
$\Delta\Delta G$= -21.9 kcal mol^{-1}

***Trans*-4,6-cyclic carbonate of protected D-mannopyranose**

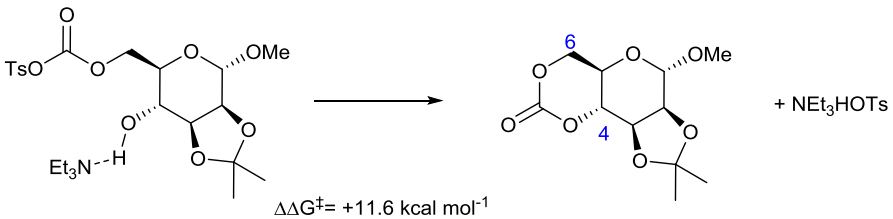

$\Delta\Delta G^{\ddagger}$= +11.6 kcal mol^{-1}
$\Delta\Delta G$= -25.8 kcal mo^{l-1}

***Trans*-4,6-cyclic carbonate of protected D-glucopyranose**

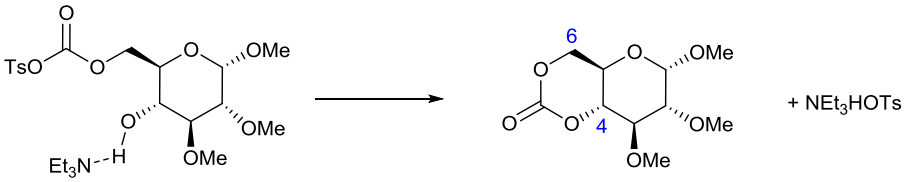

$\Delta\Delta G^{\ddagger}$= +13.7 kcal mol^{-1}
$\Delta\Delta G$= -27.1 kcal mol^{-1}

Scheme S2. Comparison of the ring-closing kinetic and thermodynamic parameters for the un-isolated *trans*-3',5'-cyclic carbonate of 3-*N*-methylthymidine and the reported *trans*-4,6-cyclic carbonates derived from D-glucose and D-mannose calculated at the rωb97xd/6-31+G(d)/cpcm=acetonitrile/298 K level of theory. 3'-Endo (^{3}E) refers to the envelope conformation of the furanose ring in the lowest energy calculated transition state. The pyranose ring in both mannose and glucose monomers adopt a $^1C_4$ chair conformation in the transition state.

	Structure	***G /Hartrees***	***ΔG/ kcalmol^{-1}***
	Trans_1	-1026.099913	
	mannoseCC	-954.883603	
	glucoseCC	-916.7632	
	HNEt3OTs	-1187.29434	
Ring-closing by nuc. add. elim. of 3'-OH at 5'-tosylcarbonate	5tosylcarbonate	-2213.361183	0.0
	5tosylcarbonate_TS	-2213.339926	+13.3
	Trans_1 + HNEt3OTs	-2383.018394	-20.8
Ring-closing by nuc. add. elim. of 3'-OH at 5'-tosylcarbonate	3tosylcarbonate	-2213.359407	0.0
	3tosylcarbonate_TS	-2213.337688	+13.6
	Trans_1 + HNEt3OTs	-2213.394253	-21.9
Mannose: Ring-closing by nuc. add. elim. of 4'-OH at 6'-tosylcarbonate	MannCarbonate	-2142.136853	0.0
	MannCarbonate_TS	-2142.118305	+11.6
	MannoseCC+HNEt3OTs	-2104.014351	-25.8
Glucose: Ring-closing by nuc. add. elim. of 4'-OH at 6'-tosylcarbonate	GluCarbonate	-2103.992447	0.0
	GluCarbonate_TS	-1850.210171	+13.7
	GlucoseCC+HNEt3OTs	-2104.05754	-27.1

Table S2. Computed Gibbs Free Energies at the rωB97XD/6-31+g(d)/cpcm=acetonitrile/298K level of theory for cyclic carbonate formation by intramolecular nucleophilic addition-elimination.

Full coordinates for all the stationary points, together with computed Gibbs free energy and vibrational frequency data, are available *via* the corresponding Gaussian 09 output files, stored in the digital repository: DOI: 10.6084/m9.figshare.4309559 .

Intramolecular "S_N2-type" Mechanism

DFT calculations at the same level of theory support experimentally findings for the formation of a 3',5'-*cis*- cyclic carbonate by backside attack of the carbonate nucleophile at the 5'-position, displacing the tosyl leaving group and inverting the stereochemistry at the 3'-position. Although, synthetically less challenging, the reverse process, attack of the carbonate at the 3'-position to displace a tosyl leaving group at the 5'-position, leading to formation of the 3',5'-*trans*-cyclic carbonate, poses a higher kinetic barrier and lower thermodynamic driving force. At this level of theory, the isolated *cis*-cyclic carbonate **1** (reported here) is 9.2 kcal mol^{-1} lower in energy compared to the theoretical and unreported *trans*-cyclic carbonate.

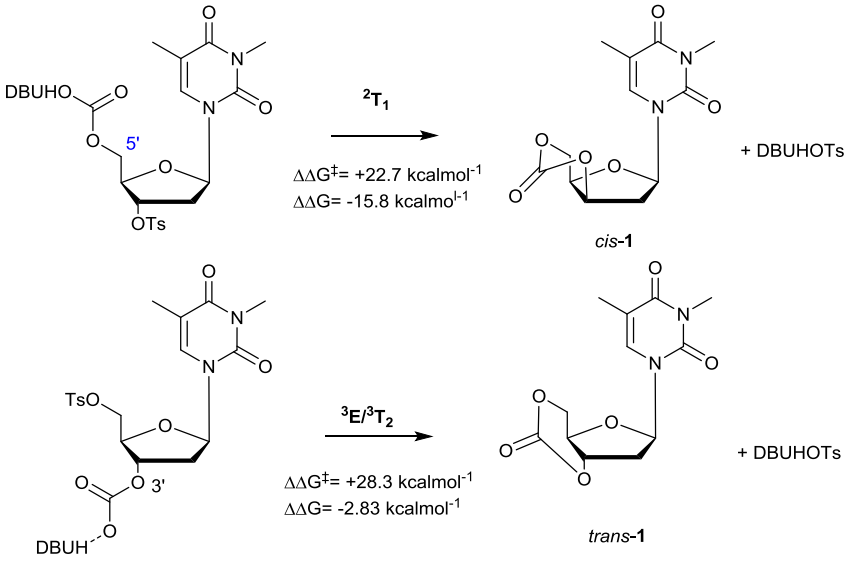

Scheme S3. Kinetic and thermodynamic parameters for ring-closing by an intramolecular displacement reaction calculated at the rωb97xd/6-31+G(d)/cpcm=acetonitrile/298 K level of theory. $^2T_1$ refers to the 2'-endo-1'-exo twist conformation of the furanose ring in the lowest energy transition state located. The input for *cis*-**1** was taken from the X-ray crystal structure data.

	Structure	***G /Hartrees***	***ΔG/ kcalmol^{-1}***
	Trans_1	-1026.099913	
	Cis_1	-1026.11592	
	DBUHOTs	-1356.918481	
Intramolecular S_N2 ring-closing with 5'-carbonate nucleophile	5carbonate3tosyl	-2383.009237	0.0
	5carbonate3tosyl_TS	-2382.97299	+22.7
	Cis_1 + DBUHOTs	-2383.034401	-15.8
Intramolecular S_N2 ring-closing with 3'-carbonate nucleophile	5tosyl3carbonate	-2383.013888	0.0
	5tosyl3carbonate_TS	-2382.968715	+28.3
	trans_1 + DBUHOTs	-2383.018394	-2.83

Table S3. Computed Gibbs Free Energies at the rωB97XD/6-31+g(d)/cpcm=acetonitrile/298K level of theory for the formation of *trans*-**1** (hypothetical) and *cis*-**1** (reported here) by intramolecular S_N2-like ring-closing with 3'- or 5'-carbonate nucleophile.

Full coordinates for all the stationary points, together with computed Gibbs free energy and vibrational frequency data, are available *via* the corresponding Gaussian 09 output files, stored in the digital repository: DOI: 10.6084/m9.figshare.4309616 .

Ring Strain

There are two prevalent methods for evaluating ring-strain: calculating the enthalpy of ring-opening with dimethyl carbonate (DMC), such that the same number of bonds are formed as broken and the Gibbs Free energy of ring-opening with primary and secondary alcohols. Ring strain calculations at the rωb97xd/6-311++G(2d,p)/cpcm=dichloromethane/298 K level of theory highlight the highly strained nature of the *trans*-configured furanose-cored monomer (*trans*-**1**) compared to the corresponding isolated *cis*-configured cyclic carbonate (*cis*-**1**). In addition, the calculations give an indication of the ROP potential of the *cis*-**1** and *cis*-**1**-Bz monomers (reported here), which form equilibrium polymerisations.

Isodesmic reaction with DMC

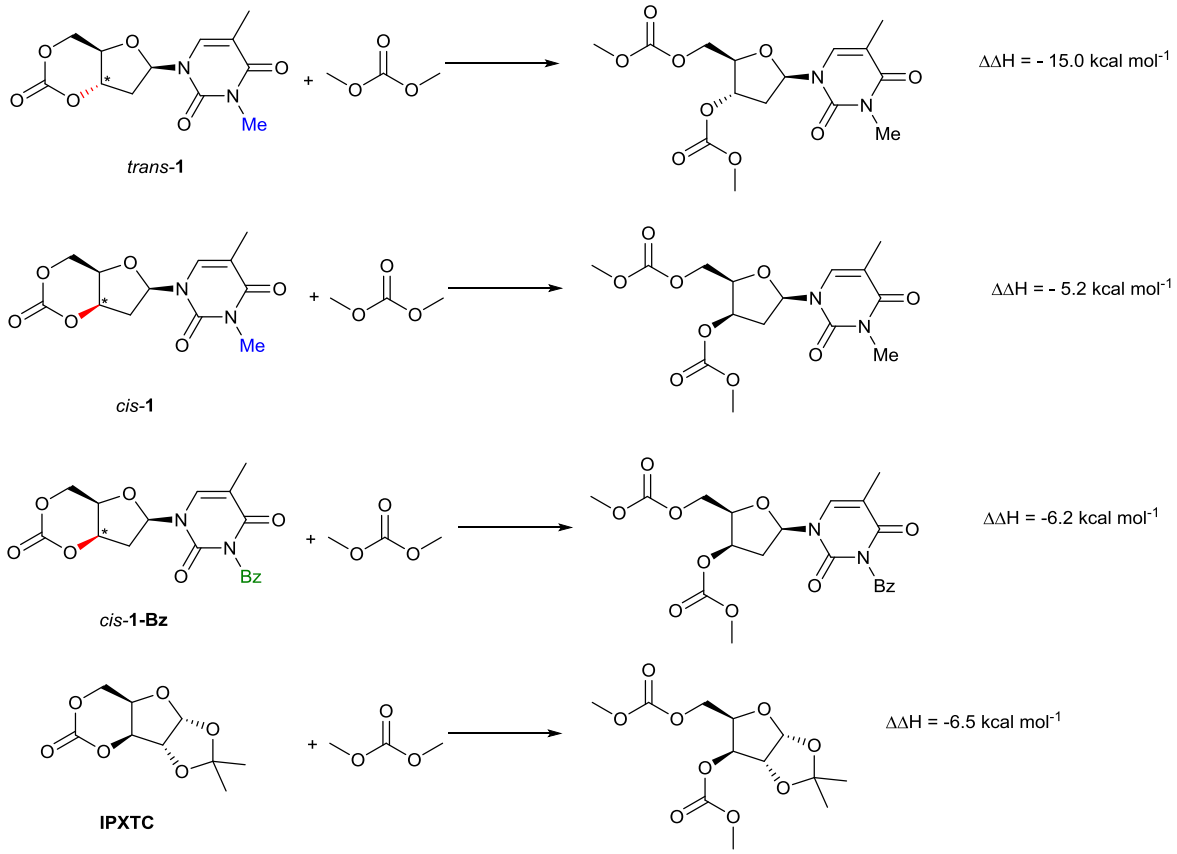

Scheme S4. Consideration of ring-stain by calculation of the enthalpy of isodesmic ring-opening with dimethyl carbonate (DMC) at rωb97xd/6-311++G(2d,p)/cpcm=dichloromethane/298 K level of theory. The synthesis and ROP of isopropylidene-D-xylofuranose-3,5-cyclic carbonate (IPXTC) was reported by Gross and coworkers.[13] Reported elsewhere[10] (and summarised in Figure S37), $\Delta\Delta H_{ring\ strain}$ for the cyclic *trans*-4,6-carbonate monomers of protected D-glucose and D-mannose sugars, at the same level of theory, are -9.8 and -9.5 kcal mol^{-1}, respectively.

	Structure	***H /Hartrees***
Starting Materials	Trans_1	-1026.301977
	Cis_1	-1026.317516
	Cis_1_Bz	-1331.296124
	xyloseCC	-801.309791
	DMC	-343.512814
Products	DMC_Trans_1	-1369.838650
	DMC_Cis_1	-1369.838544
	Cis_1_Bz	-1674.818767
	DMC_xylose	-1144.832963

Table S4. Computed Gibbs Free Energies at the rωB97XD/6-311++g(2d,p)/cpcm=dichloromethane/298K level of theory for the isodesmic ring-opening with dimethyl carbonate (DMC) of *trans*-**1**, *cis*-**1,** cis-**1**-**Bz** and IPXTC. The values for the glucose and mannose monomers have been reported previously.[10]

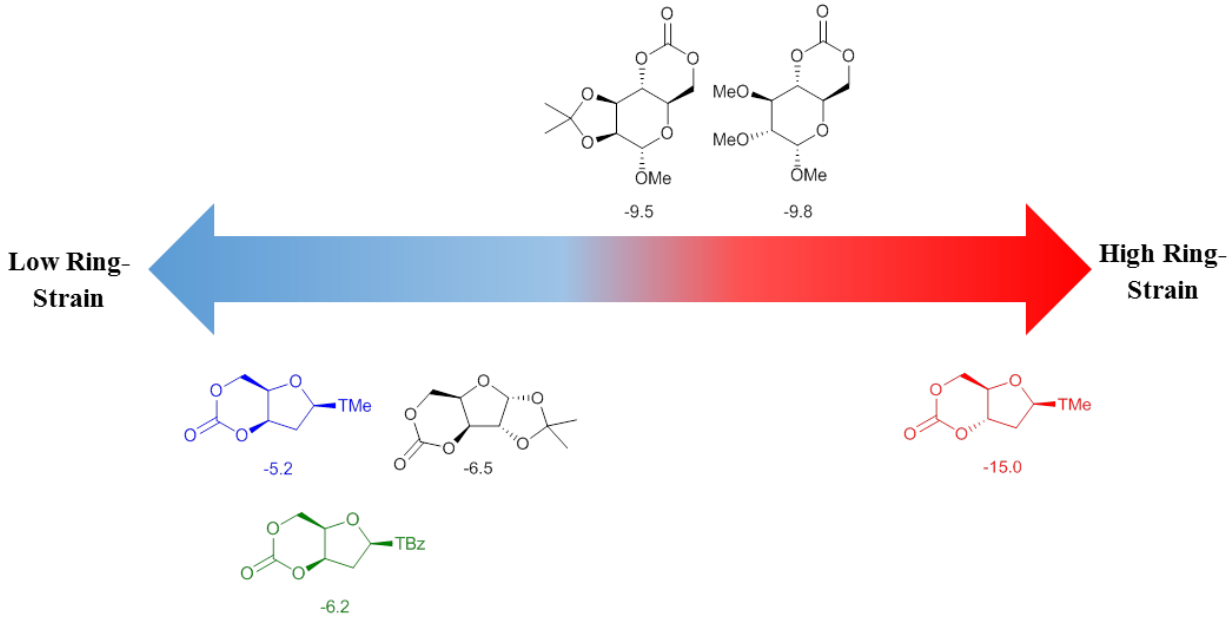

Figure S36. Illustrative summary of calculated enthalpies (ΔΔH) for ring-opening with DMC performed at the rωb97xd/6-311++G(2d,p)/cpcm=dichloromethane/298 K level of theory.

Full coordinates for all the stationary points, together with computed Gibbs free energy and vibrational frequency data, are available *via* the corresponding Gaussian 09 output files, stored in the digital repository: DOI: 10.6084/m9.figshare.4309469 .

Thermodynamics of Ring-Opening with MeOH and ^{i}PrOH

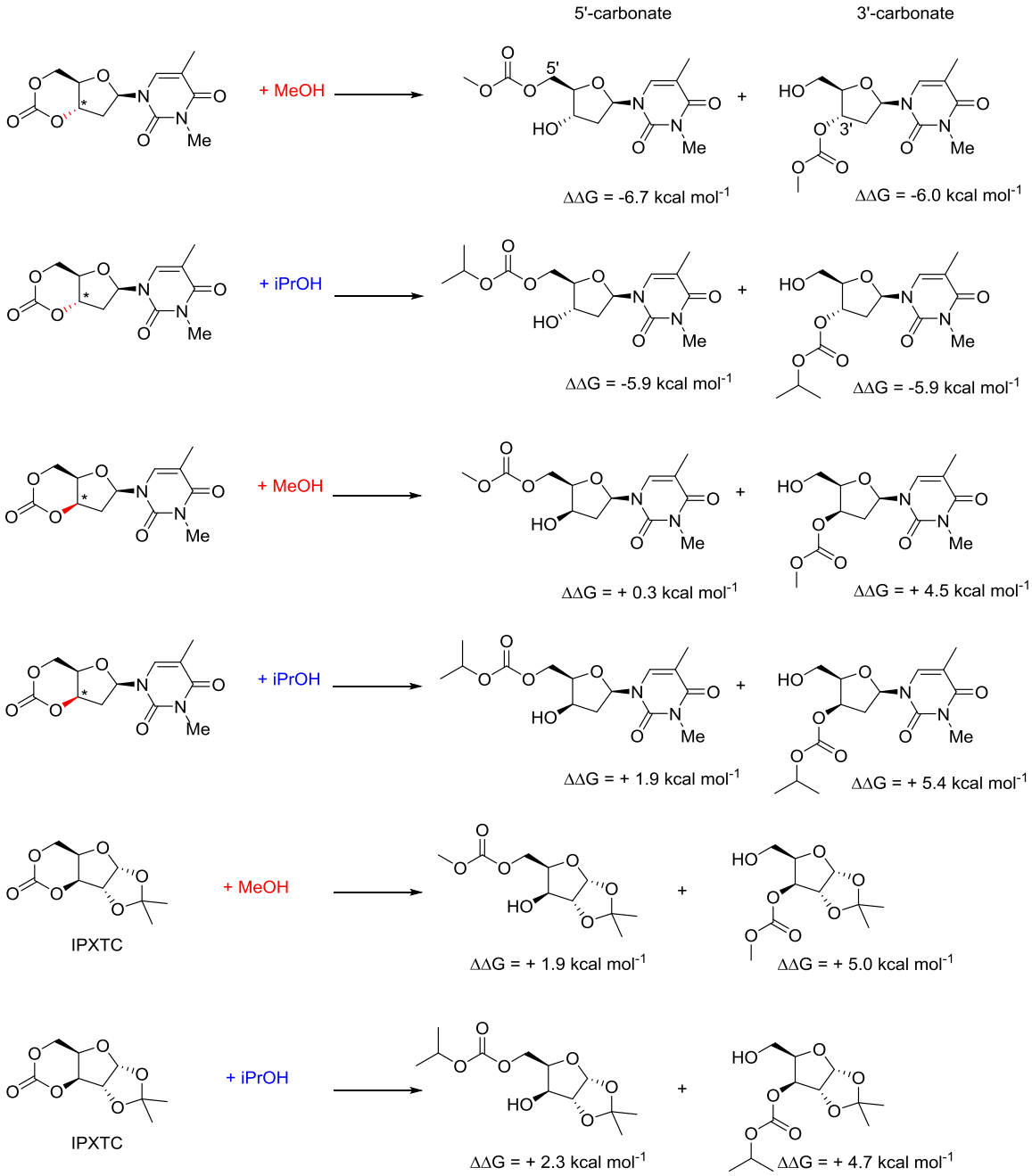

Scheme S5. Gibbs Free energy (ΔΔG) for the ring-opening of *cis*-**1** (reported here) and *trans*-**1** (hypothetical) with primary and secondary alcohols computed at the rωb97xd/6-311++G(2d,p)/cpcm=dichloromethane/298 K level of theory. The synthesis and ROP of isopropylidene-D-xylofuranose-3,5-cyclic carbonate (IPXTC) (calculated for comparison) was reported by Gross and coworkers.[13] Reported previously[10] (and summarised in Figure S38), at the same level of theory, ring-opening with MeOH of the *trans*-4,6-cyclic carbonate monomer derived from D-mannose to place the carbonate at the primary or secondary positions was -0.9 and +3.9 kcal mol^{-1}, respectively and for the corresponding D-glucose cyclic carbonate -0.2 and +2.8 kcal mol^{-1}.

	Structure	***G /Hartrees***	***ΔG/ kcalmol^{-1}***
Starting Materials	Trans_1	-1026.367241	
	Cis_1	-1026.381294	
	xyloseCC	-801.362796	
	MeOH	-115.702205	
	iPrOH	-194.286844	
Trans-**1**	Trans_1+ MeOH	-1142.069446	0.0
	MeOH_trans1_3	-1142.080069	-6.7
	MeOH_trans1_5	-1142.079064	-6.0
	Trans_1 + iPrOH	-1220.654085	0.0
	PrOH_trans1_3	-1220.66344	-5.9
	PrOH_trans1_5	-1220.66355	-5.9
Cis-**1**	cis_1+ MeOH	-1142.083499	0.0
	MeOH_cis1_3	-1142.07635	4.5
	MeOH_cis1_5	-1142.083087	0.3
	cis_1 + iPrOH	-1220.668138	0.0
	PrOH_cis1_3	-1220.659461	5.4
	PrOH_ cis1_5	-1220.665093	1.9
IPXTC	xyloseCC+ MeOH	-917.065001	0.0
	MeOH_xylose_3	-917.057093	5.0
	MeOH_xylose_5	-917.061942	1.9
	xyloseCC+ iPrOH	-995.64964	0.0
	PrOH_xylose_3	-995.64208	4.7
	PrOH_xylose_5	-995.646029	2.3

Table S5. Computed Gibbs Free Energies at the rωB97XD/6-311++g(2d,p)/cpcm=dichloromethane/298K level of theory for the ring-opening of *trans*-**1**, *cis*-**1** and IPXTC. The values for the glucose and mannose monomers have been reported previously.[10]

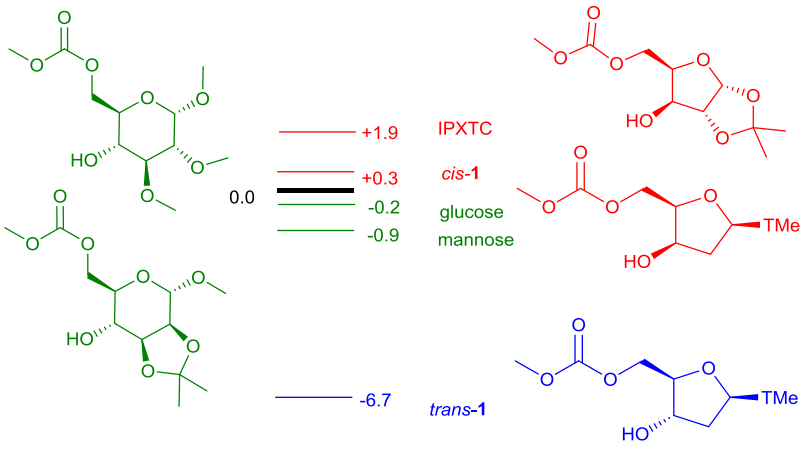

Figure S37. Illustrative overview of calculated ring-opening thermodynamics for sugar-based cyclic carbonates at the rωb97xd/6-311++G(2d,p)/cpcm=dichloromethane/298 K level of theory. Only ring-opening with MeOH to give a primary carbonate is shown.

Full coordinates for all the stationary points, together with computed Gibbs free energy and vibrational frequency data, are available *via* the corresponding Gaussian 09 output files, stored in the digital repository: DOI: 10.6084/m9.figshare.4309487 .

Initiation Step for the ROP of 1 with TBD and 4-MeBnOH

The thermodynamics and kinetics of the initial ring-opening of **1** with TBD organocatalyst and 4-MeBnOH initiator were considered. A higher basis set, the split-valence triple ζ with polarisation *and* diffuse functions, 6-311++G(d,p) was used for the carbonate, guanidine and alcohol moieties of **1**, TBD and 4-MeBnOH, respectively and the lower, split-valence double ζ 6-31+g(d) basis set was applied to the rest. This mixture of basis sets was selected to account for potential anions and non-bonding (hydrogen bonding) interactions, while allowing the models to scale up to the maximum size of 76 atoms. Only attack of the 4-methylbenzyl alcohol at the face opposite to the bulky thymine nucleobase was considered.

Explicitly considering the TBD catalyst and 4-MeBnOH initiator, ring-opening of **1** is both thermodynamically and kinetically favourable. The highest kinetic barrier calculated is just 9.2 kcal mol^{-1} and correlates to migration of the TBD. Ring-opening to expose either a primary or secondary alcohol for chain growth is downhill by -5.6 or -6.6 kcal mol^{-1}, respectively. This lack of preference to open to either side of the asymmetric monomer supports the formation of regiorandom polymer.

Full coordinates for all the stationary points, together with computed Gibbs free energy and vibrational frequency data, are available *via* the corresponding Gaussian 09 output files, stored in the digital repository: DOI: 10.6084/m9.figshare.4309430 .

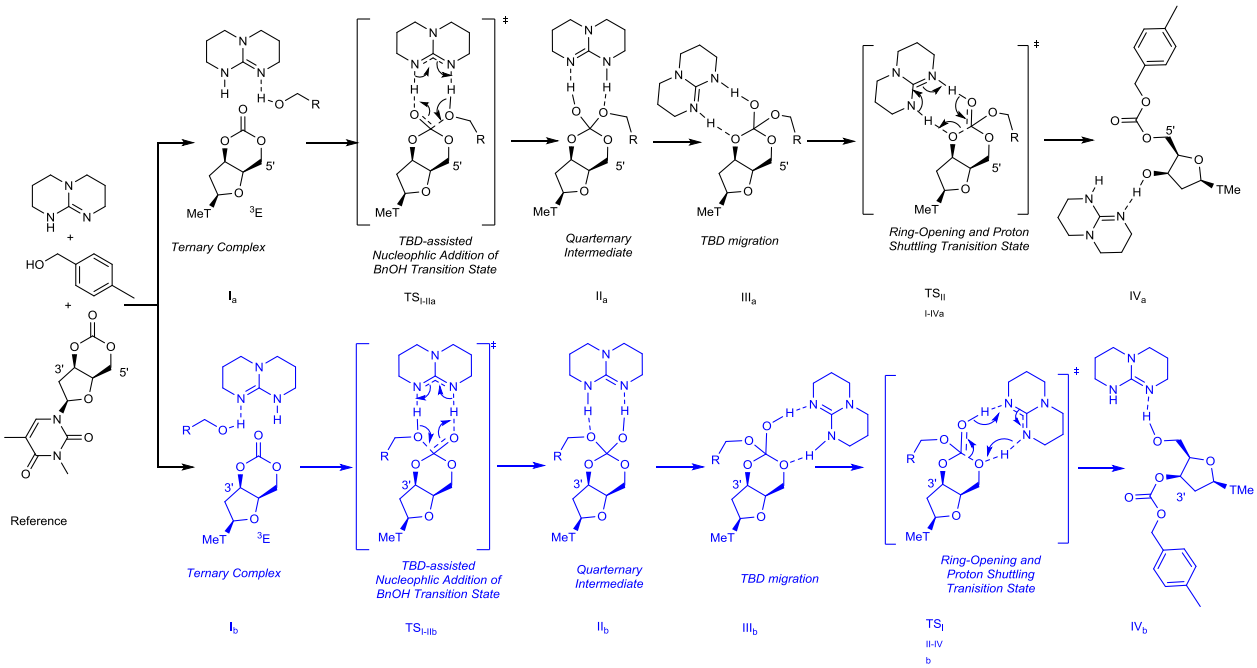

Scheme S6. Intermediates and transition states calculated for the initiation step in the ROP of **1** with 4-MeBnOH and TBD catalyst.

	Structure	***G /Hartrees***	***ΔG/ kcalmol^{-1}***
Starting Materials	**1**	-1025.912381	
	TBD	-438.513199	
	4MeBnOH	-385.796245	
	Reference	**-1850.221825**	**0**
Ring-opening to free secondary OH (carbonate on primary)	I_a	-1850.222786	-0.6
	TS_{I-IIa}	-1850.210771	+6.9
	II_a	-1850.223471	-1.0
	III_a	-1850.231710	-6.2
	$TS_{III-IVa}$	-1850.217115	+3.0
	IV_a	-1850.230724	-5.6
Ring-opening to free primary OH (carbonate on secondary)	I_b	-1850.222285	-0.3
	TS_{I-IIb}	-1850.210171	+7.3
	II_b	-1850.223610	-1.1
	III_b	-1850.225922	-2.6
	$TS_{III-IVb}$	-1850.213885	+5.0
	IV_b	-1850.232327	-6.6

Table S6. Computed Gibbs Free Energies at the rωB97XD/6-311+g(d,p)/6-31+g(d)/cpcm=dichloromethane/298K level of theory for the ring-opening of **1** with 4-methylbenzyl alcohol initiator and TBD catalyst.

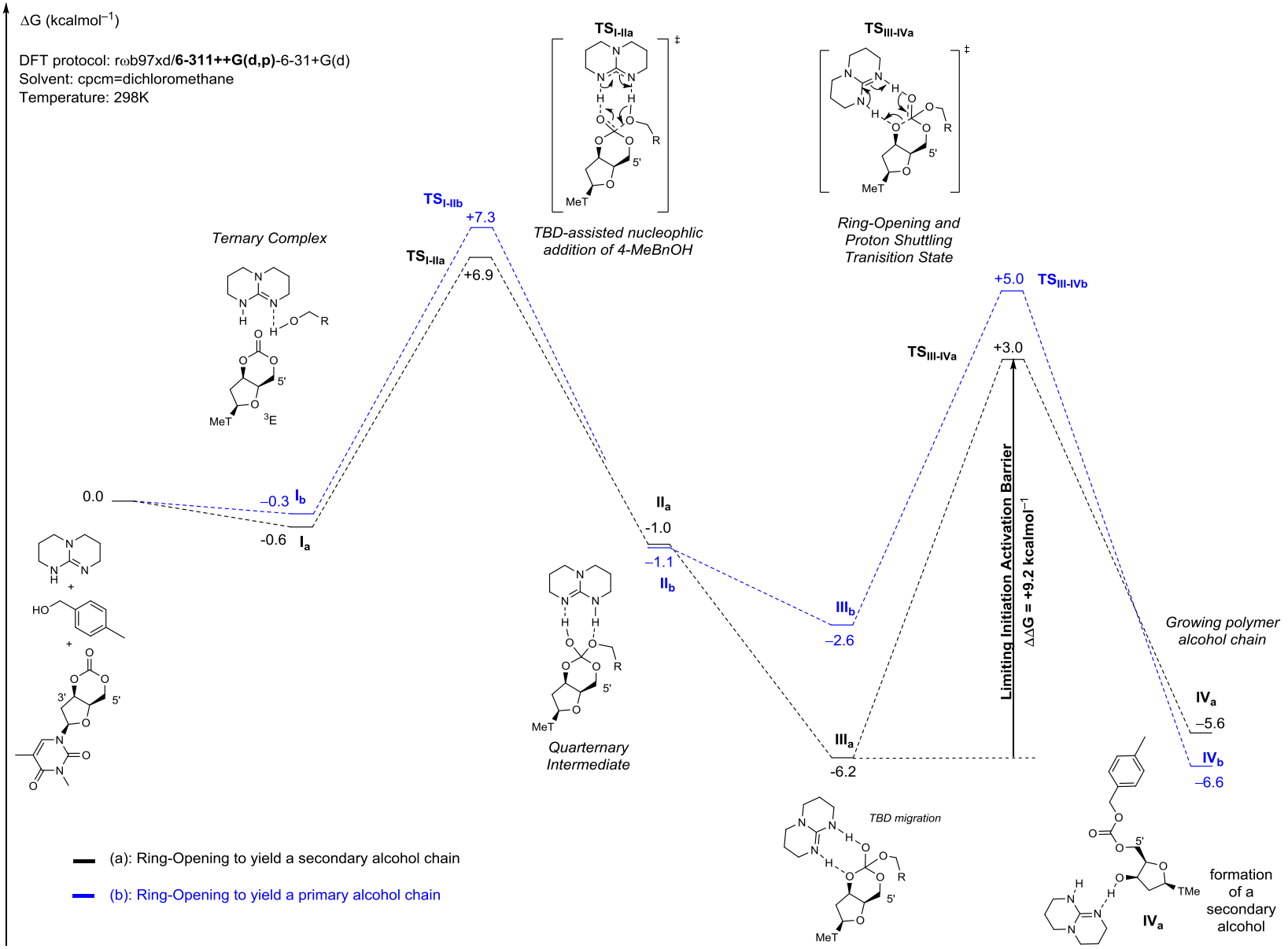

Figure S38. DFT computations for the initiation step in the ROP of **1** with 4-MeBnOH and TBD catalyst. Little difference is observed between ring-opening to expose either a free secondary or primary hydroxyl group for chain propagation; the main difference lying in the TBD migration intermediates III_a and III_b due to the β-anomeric nucleobase.

12. Single Crystal X-ray Diffraction Data

Cyclic 3-N-methyl-3',5'-O-cis-carbonate-thymidine (1)

Empirical formula	$C_{12}H_{14}N_2O_6$	
Formula weight	282.25	
Temperature	150(2) K	
Wavelength	1.54184 Å	
Crystal system	Monoclinic	
Space group	$P2_1$	
Unit cell dimensions	a = 7.0627(2) Å	α= 90°.
	b = 9.6573(4) Å	β= 110.448(4)°.
	c = 10.0320(3) Å	γ = 90°.
Volume	641.13(4) $Å^3$	
Z	2	
Density (calculated)	1.462 Mg/m^3	
Absorption coefficient	1.016 mm^{-1}	
F(000)	296	
Crystal size	0.300 x 0.100 x 0.020 mm^3	
Theta range for data collection	6.572 to 72.400°.	
Index ranges	-7<=h<=8, -11<=k<=9, -11<=l<=12	
Reflections collected	5532	
Independent reflections	2172 [R(int) = 0.0267]	
Completeness to theta = 67.684°	99.6 %	
Absorption correction	Semi-empirical from equivalents	
Max. and min. transmission	1.00000 and 0.78559	
Refinement method	Full-matrix least-squares on F^2	
Data / restraints / parameters	2172 / 1 / 183	
Goodness-of-fit on F^2	1.060	
Final R indices [I>2sigma(I)]	R1 = 0.0314, wR2 = 0.0779	
R indices (all data)	R1 = 0.0330, wR2 = 0.0792	
Absolute structure parameter	0.01(11)	
Extinction coefficient	n/a	
Largest diff. peak and hole	0.139 and -0.175 $e.Å^{-3}$	

3-N-methyl-3'-tosyl-thymidine (2)

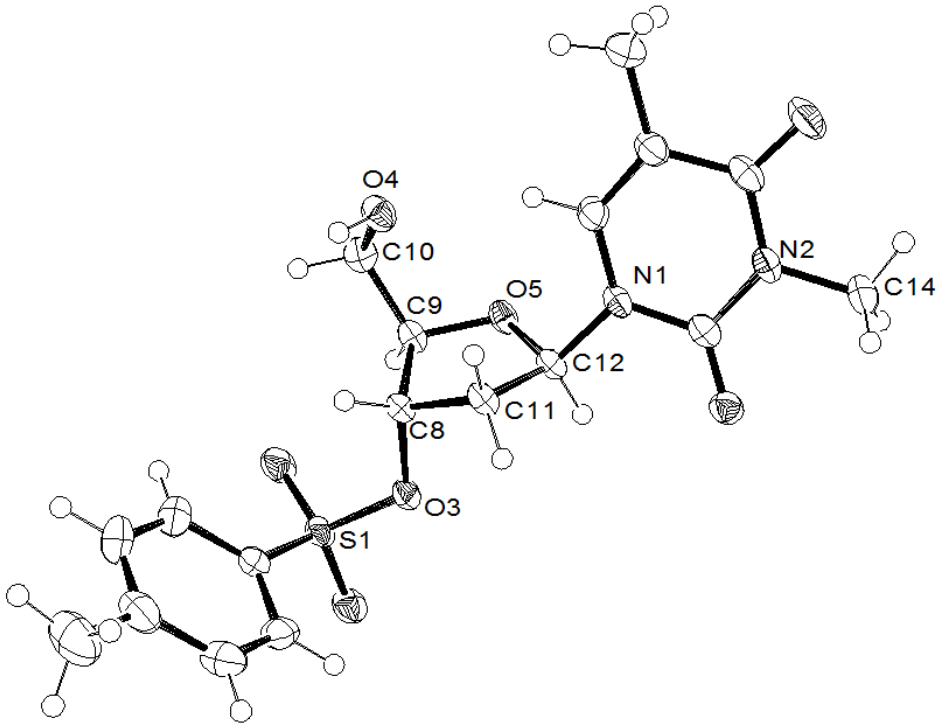

Empirical formula	$C_{18}H_{22}N_2O_7S$	
Formula weight	410.43	
Temperature	150(2) K	
Wavelength	1.54184 Å	
Crystal system	Monoclinic	
Space group	$P2_1$	
Unit cell dimensions	a = 6.44190(10) Å	α= 90°.
	b = 14.7348(2) Å	β= 106.3100(10)°.
	c = 10.71760(10) Å	γ = 90°.
Volume	976.37(2) $Å^3$	
Z	2	
Density (calculated)	1.396 Mg/m^3	
Absorption coefficient	1.859 mm^{-1}	
F(000)	432	
Crystal size	0.200 x 0.100 x 0.080 mm^3	
Theta range for data collection	4.298 to 72.553°.	
Index ranges	-7<=h<=7, -18<=k<=17, -12<=l<=12	
Reflections collected	14552	
Independent reflections	3741 [R(int) = 0.0372]	

Completeness to theta = 67.684°	99.9 %
Absorption correction	Semi-empirical from equivalents
Max. and min. transmission	1.00000 and 0.52689
Refinement method	Full-matrix least-squares on F^2
Data / restraints / parameters	3741 / 1 / 260
Goodness-of-fit on F^2	1.045
Final R indices [I>2sigma(I)]	R1 = 0.0286, wR2 = 0.0736
R indices (all data)	R1 = 0.0293, wR2 = 0.0742
Absolute structure parameter	-0.003(8)
Extinction coefficient	n/a
Largest diff. peak and hole	0.135 and -0.342 e.$Å^{-3}$

13. References

[1] J. Adams, M. David and R. W. Giese, *Anal. Chem.*, 1986, **58**, 345-348.

[2] J. Adams, M. David and R. W. Giese, *Anal. Chem.*, 1986, **58**, 345-348.

[3] A. Buchard, F. Jutz, M. R. Kember, A. J. P. White, H. S. Rzepa and C. K. Williams, *Macromolecules*, 2012, **45**, 6781-6795.

[4] J.-D. Chai and M. Head-Gordon, *Phys. Chem. Chem. Phys.* , 2008, **10**, 6615-6620.

[5] J.-D. Chai and M. Head-Gordon, *J. Chem. Phys.*, 2008, **128**, 084106.

[6] B. M. Chamberlain, M. Cheng, D. R. Moore, T. M. Ovitt, E. B. Lobkovsky and G. W. Coates, *J. Am. Chem. Soc.*, 2001, **123**, 3229-3238.

[7] M. Cheng, A. B. Attygalle, E. B. Lobkovsky and G. W. Coates, *J. Am. Chem. Soc.*, 1999, **121**, 11583-11584.

[8] M. Cossi, N. Rega, G. Scalmani and V. Barone, *J. Comput. Chem.*, 2003, **24**, 669-681.

[9] M. J. Frisch, G. W. Frucks, H. B. Schlegel, G. E. Scuseria, M. A. Robb, J. R. Cheeseman, G. Scalmani, V. Barone, B. Mennucci, G. A. Petersson, H. Nakatsuji, M. Caricato, X. Li, H. P. Hratchian, A. F. Izmaylov, J. Bloino, G. Zheng, J. L. Sonnenberg, M. Hada, M. Ehara, K. Toyota, R. Fukuda, J. Hasegawa, M. Ishida, T. Nakajima, Y. Honda, O. Kitao, H. Nakai, T. Vreven, J. Montgomery, J. A.;, J. E. Peralta, F. Ogliaro, M. Bearpark, J. J. Heyd, E. Brothers, K. N. Kudin, V. N. Staroverov, R. Kobayashi, J. Normand, K. Raghavachari, A. Rendell, J. C. Burant, S. S. Iyengar, J. Tomasi, M. Cossi, N. Rega, J. M. Millam, M. Klene, J. E. Knox, J. B. Cross, V. Bakken, C. Adamo, J. Jaramillo, R. Gomperts, R. E. Stratmann, O. Yazyev, A. J. Austin, R. Cammi, C. Pomelli, J. W. Ochterski, R. L. Martin, K. Morokuma, V. G. Zakrzewski, G. A. Voth, P. Salvador, J. J. Dannenberg, S. Dapprich, A. D. Daniels, Ö. Farkas, J. B. Foresman, J. V. Ortiz, J. Cioslowski and D. J. Fox, Gaussian 09 (Revision D.01), Gaussian, Inc., Wallingford CT, 2009.

[10] G. L. Gregory, L. M. Jenisch, B. Charles, G. Kociok-Köhn and A. Buchard, *Macromolecules*, 2016, **49**, 7165-7169.

[11] E. Larsen, T. Kofoed and E. B. Pedersen, *Synthesis*, 1995, **1995**, 1121-1125.

[12] G. Scalmani and M. J. Frisch, *J. Chem. Phys.*, 2010, **132**, 114110.

[13] Y. Shen, X. Chen and R. A. Gross, *Macromolecules*, 1999, **32**, 2799-2802.

[14] A. R. Vaino and W. A. Szarek, *Chem. Comm.*, 1996, 2351-2352.

[15] C. K. Williams, L. E. Breyfogle, S. K. Choi, W. Nam, V. G. Young, M. A. Hillmyer and W. B. Tolman, *J. Am. Chem. Soc.*, 2003, **125**, 11350-11359.

[16] D. M. York and M. Karplus, *J. Phys. Chem. A*, 1999, **103**, 11060-11079.